Development 139, 3373-3382 (2012) doi:10.1242/dev.083873

BMP-dependent serosa and amnion specification in the scuttle fly *Megaselia abdita*

Ab. Matteen Rafiqi*, Chee-Hyurng Park§, Chun Wai Kwan§, Steffen Lemke‡ and Urs Schmidt-Ott¶

SUMMARY

Bone morphogenetic protein (BMP) signaling is an essential factor in dorsoventral patterning of animal embryos but how BMP signaling evolved with fundamental changes in dorsoventral tissue differentiation is unclear. Flies experienced an evolutionary reduction of extra-embryonic tissue types from two (amniotic and serosal tissue) to one (amnionserosal tissue). BMP-dependent amnioserosa specification has been studied in *Drosophila melanogaster*. However, the mechanisms of serosal and amniotic tissue specification in less diverged flies remain unknown. To better understand potential evolutionary links between BMP signaling and extra-embryonic tissue specification, we examined the activity profile and function of BMP signaling in serosa and amnion patterning of the scuttle fly *Megaselia abdita* (Phoridae) and compared the BMP activity profiles between *M. abdita* and *D. melanogaster*. In blastoderm embryos of both species, BMP activity peaked at the dorsal midline. However, at the beginning of gastrulation, peak BMP activity in *M. abdita* shifted towards prospective amnion tissue. This transition correlated with the first signs of amnion differentiation laterally adjacent to the serosa anlage. Marker-assisted analysis of six BMP signaling components (*dpp*, *gbb*, *scw*, *tkv*, *sax*, *sog*) by RNA interference revealed that both serosa and amnion specification of *M. abdita* are dependent on BMP activity. Conversely, BMP gain-of-function experiments caused sharpened expression boundaries of extra-embryonic target genes indicative of positive feedback. We propose that changes in the BMP activity profile at the beginning of gastrulation might have contributed to the reduction of extra-embryonic tissue types during the radiation of cyclorrhaphan flies.

KEY WORDS: Evolutionary development, Bone morphogenetic protein, Diptera

INTRODUCTION

Bone morphogenetic proteins (BMPs) are important players in the dorsoventral differentiation of animal embryos (Niehrs, 2010), but how BMP signaling evolves with changes in tissue specification is not well understood. Flies (Diptera) provide an excellent opportunity to address this question because the BMP pathway of *Drosophila melanogaster* embryos has been studied in much detail (O'Connor et al., 2006; Umulis et al., 2009) and because extra-embryonic tissue specification, presumably under the control of the BMP pathway, has changed in dipteran evolution (Fig. 1) (Schmidt-Ott et al., 2010). Schizophoran flies, which include *D. melanogaster*, develop a single extra-embryonic tissue called the amnioserosa. This tissue is specified along the dorsal midline of the blastoderm and closes the dorsal side of the germband. In non-schizophoran dipterans, dorsal blastoderm folds over the gastrulating embryo and differentiates into two tissues: a cuticle-secreting serosa underneath the eggshell and an amnion that either lines the ventral side or closes the dorsal side of the germband (Goltsev et al., 2007; Rafiqi et al., 2008; Goltsev et al., 2009). Dorsal patterning of the dipteran embryo must have changed with the evolutionary transition from two extra-embryonic tissue types to one, but whether the transition involved altered BMP activity or genetic changes downstream or independent of this signaling pathway is unknown.

University of Chicago, Department of Organismal Biology and Anatomy, CLSC 1061C, 920 E. 58th Street, Chicago, IL 60637, USA.

*Present address: McGill University, Department of Biology, 1205 Dr Penfield Avenue, Montréal, Québec, H3A 1B1, Canada
‡Present address: University of Heidelberg, Centre for Organismal Studies, Im Neuenheimer Feld 230, 69120 Heidelberg, Germany
§These authors contributed equally to this work
¶Author for correspondence (uschmid@uchicago.edu)

Accepted 21 June 2012

In *D. melanogaster*, high levels of BMP activity are required to induce amnioserosa formation (Ray et al., 1991; Arora and Nusslein-Volhard, 1992; Ferguson and Anderson, 1992a; Wharton et al., 1993). This activity is induced by the extracellular ligands Decapentaplegic (Dpp) and Screw (Scw) (Padgett et al., 1987; Arora et al., 1994; Shimmi et al., 2005), which are secreted into the perivitelline space and transported in the presence of antagonists towards the dorsal midline (Francois et al., 1994; Ashe and Levine, 1999; Decotto and Ferguson, 2001; Eldar et al., 2002; Shimmi et al., 2005; Wang and Ferguson, 2005). Dorsally, BMP dimers are released from their antagonists to the transmembrane receptor proteins Thickveins (Tkv) and Saxophone (Sax), triggering phosphorylation of the transcription factor Mad and thereby BMP-dependent transcriptional gene regulation (Shimell et al., 1991; Ferguson and Anderson, 1992b; Marques et al., 1997; Shimmi et al., 2005; Wang and Ferguson, 2005). The BMP transport and release mechanism results in a shallow gradient of BMP activity, which broadly influences patterning in the dorsal ectoderm (Mizutani et al., 2006). Through a positive-feedback loop, the initially shallow gradient of BMP activity is transformed into a narrow and sharply delineated domain of high BMP activity (Wang and Ferguson, 2005; Umulis et al., 2006; Umulis et al., 2010), which, at this stage, becomes crucial for the expression of *zerknüllt* (*zen*) and hence amnioserosa specification (Rushlow et al., 2001; Liang et al., 2008). Dpp is essential for BMP activity and therefore controls the specification of all tissues that develop under the control of the BMP pathway in the early embryo, including the amnioserosa and dorsal ectoderm (Ferguson and Anderson, 1992b; Wharton et al., 1993). *scw*, a diverged paralog of *glass bottom boat* (*gbb*) (Van der Zee et al., 2008; Fritsch et al., 2011), boosts BMP activity along the dorsal midline and is required to generate high BMP activity for amnioserosa specification (Arora et al., 1994).

Functional data on the BMP pathway components of dipterans other than *D. melanogaster* are currently unavailable, but orthologs of many specific BMP signaling components of *D. melanogaster* have been identified in other cyclorrhaphan flies (Fritsch et al., 2011; Lemke et al., 2011). Using an antibody against pMad (the phosphorylated, activated BMP signal transducer), it has been shown that, in the mosquito *Anopheles gambiae*, BMP activity covers a much broader area of the dorsal blastoderm than in *D. melanogaster* (Goltsev et al., 2007). This difference correlates with clearly distinct expression patterns of *short gastrulation* (*sog*) and *tolloid* (*tld*), which encode extracellular BMP signaling components. Sog (a homolog of vertebrate chordin) functions as an antagonist of BMP dimers (Francois et al., 1994; Biehs et al., 1996; Marques et al., 1997; Shimmi et al., 2005). Tld, a metalloprotease, cleaves Sog and allows BMP dimers to bind their receptors (Marques et al., 1997; Shimmi et al., 2005; Wang and Ferguson, 2005).

In *D. melanogaster*, *sog* is expressed laterally in the neurogenic ectoderm, whereas in *A. gambiae* it is expressed ventrally in the prospective mesoderm [as in beetles (van der Zee et al., 2006)]. The difference in *sog* expression could explain the comparatively broad pMad domain in *A. gambiae* embryos. Furthermore, in *D. melanogaster*, *tld* is expressed on the dorsal side of the blastoderm embryo in non-neurogenic ectoderm (Shimell et al., 1991), whereas in *A. gambiae* it is expressed more broadly but, notably, is repressed in a region that roughly corresponds to the serosa anlage. As the activity pattern of *tld*, in *D. melanogaster* at least, seems to be tied to its local transcription (Wang and Ferguson, 2005), the difference in *tld* expression between *D. melanogaster* and *A. gambiae* suggests that the prospective amnion, rather than the serosa, receives peak levels of BMP activity in the *A. gambiae* embryo. Yet, according to the authors of the mosquito study, pMad in the mosquito blastoderm peaks along the dorsal midline. They therefore proposed that laterally released BMP dimers accumulate along the dorsal midline, generating peak levels there. The resulting BMP activity gradient would specify serosal tissue at peak levels and amniotic tissue at a lower activity threshold (Goltsev et al., 2007). However, this model does not account for the fact that, immediately posterior to the serosa anlage, prospective amnion tissue straddles the dorsal midline.

Here we provide an analysis of BMP signaling in the scuttle fly *Megaselia abdita* (Phoridae). We chose this species because it is a close outgroup of amnioserosa-forming schizophoran flies, it is amenable to functional studies and easily maintained in culture, and because its egg size and embryonic development are very similar to those of *D. melanogaster*. We describe dynamic changes in BMP activity at the beginning of gastrulation that correlate with early signs of amnion specification. Furthermore, we show that both amnion and serosa patterning are dependent on BMP activity, and that BMP activity in *M. abdita* embryos is subject to positive feedback. Our findings are summarized in a new model of serosa and amnion specification.

MATERIALS AND METHODS

Flies and cloning procedures

Megaselia abdita Schmitz and *Drosophila melanogaster* (Oregon strain) were reared in the laboratory. Partial open reading frames of *M. abdita* (*Mab*) homologs were cloned into pCRII-TOPO vector (Invitrogen) using degenerate and specific PCR primers as follows (5′-3′): *Mab-dpp*, TNTAYGCNSARATHATGGGNCA and GGNGCNACDATCCARTC; *Mab-gbb*, AARTCNGCNCCNMARTWYYT and NGCRTGRTTNGTNGCRTTCATRTG; *Mab-scw*, TTCCTAACCATCGTCAGCAAGC and CAACAAATTTATTAACAATTAAAAGCC; *Mab-sax*, TGYCARAAYGCNATHCARTGYTGG and RTTYTGRTGCCARCAYTCYTTCAT; *Mab-tkv*, GGNGARGTNTGGYTNGCNAARTGG and TGCCARCAYTCYTGCATDATYTT; *Mab-sog*, CCNCCNTTYGGNGTNATGTAYTG and YTCYARYAGNGARCTRAANARYTC; followed by a half nested reaction using as a substitute for the first primer CARTGYMGNAAYATNAARAAYGA.

In situ hybridization, immunohistochemistry, RNAi and mRNA injections

For single-color in situ hybridization, *M. abdita* embryos were collected, heat fixed and hybridized as described (Rafiqi et al., 2008; Rafiqi et al., 2011). Antisense RNA probes were prepared from the linearized pCRII-TOPO plasmids of the PCR clones and labeled with digoxigenin or FITC as described (Tautz and Pfeifle, 1989; Kosman et al., 2004). For immunostaining and double in situ hybridization, *D. melanogaster* and *M. abdita* embryos were fixed by the slow formaldehyde fixing method using PEMS (100 mM PIPES, 2 mM $MgSO_4$, 1 mM EGTA) (pH 6.9) (Rothwell and Sullivan, 2000). For *M. abdita*, a 3:1 PEMS:methanol solution was used instead of PEMS, and formaldehyde was used at a final concentration of 5% instead of 4%. These embryos were treated with proteinase K in PBS at a final concentration of 0.08 U/ml (1 hour on ice for in situ hybridizations; 2 minutes at room temperature for pMad immunohistochemistry) and postfixed in 5% formaldehyde in PBT (0.1% Tween 20 in PBS) for 25 minutes. The proteinase K treatment was necessary to reduce species-specific background of the pMad antiserum in *M. abdita* embryos. Double in situ hybridizations with probes against *Mab-zen* and *Mab-hnt* transcripts were performed with digoxigenin (DIG)-labeled and fluorescein (FITC)-labeled probes, and detected with Fab fragments from anti-FITC or anti-DIG antibodies conjugated with alkaline phosphatase (AP; Roche, Indianapolis, IN, USA). AP activity was detected with nitroblue tetrazolium and 5-bromo-4-chloro-3-indolyl phosphate (NBT/BCIP) (Roche), which produce a dark blue precipitate, or with VectorRed (Vector Labs, Burlingame, CA, USA), which produces red precipitate and a fluorescent signal in the Cy3 channel. Double in situ hybridizations with probes against *Mab-eve* and *Mab-zen* or *Mab-hnt* transcripts were performed with biotin-labeled and FITC-labeled probes, respectively. Biotin was detected with mouse anti-biotin IgG and Alexa Fluor 488-conjugated sheep anti-mouse IgG (Jackson ImmunoResearch, West Grove, PA, USA). FITC was detected with rabbit anti-FITC IgG and Cy3-conjugated donkey anti-rabbit IgG (Jackson ImmunoResearch). pMad was detected with rabbit antiserum against the phosphopeptide NH2-CNPIS-S[PO3]-V-S[PO3]-COOH, which was generated by Dan Vasiliauskas, Susan Morton, Tom Jessell and Ed Laufer and kindly provided by Ed Laufer (Columbia University, New York, NY, USA), biotinylated goat anti-rabbit IgG (Vector Labs), and AP-conjugated anti-biotin Fab fragments (Roche). For pMad quantifications, we used Cy3-conjugated donkey anti-rabbit IgG (Jackson ImmunoResearch).

Capped mRNAs of *tkv*, *tkv-a* and *noggin* were prepared from available pSP35T plasmids (Holley et al., 1996; Neul and Ferguson, 1998) using SP6 polymerase with the mMessage mMachine Kit (Ambion). mRNA was prepared at 3 μg/μl (*tkv*, *tkv-a*) or 5 μg/μl (*noggin*). Embryos were injected at the syncytial blastoderm stage (~1:40 to 2:45 hours after egg deposition), and fixed at late blastoderm stage or shortly after the onset of gastrulation. RNA interference (RNAi) was performed as described (Rafiqi et al., 2008; Rafiqi et al., 2010).

Staging of embryos

For consistent staging of both *Megaselia* and *Drosophila* embryos, morphological landmarks were measured from sagittal views of Nomarski images using ImageJ software (Schneider et al., 2012). Progression of blastoderm cellularization was approximated by dividing the distance from the apical cell membrane to the cellularization front (d1) by the distance of the apical cell membrane to the basal side of the nuclear envelope (d2) and dividing the d1/d2 coefficient by 2. Accordingly, the time point when the apicobasal level of the cellularization front coincided with the basal side of blastoderm nuclei was treated as 50% blastoderm cellularization. Ventral furrow formation (mesoderm invagination) and cephalic furrow formation were used as markers to determine the beginning of gastrulation. The onset of pole cell migration was variable. After cephalic furrow formation, we

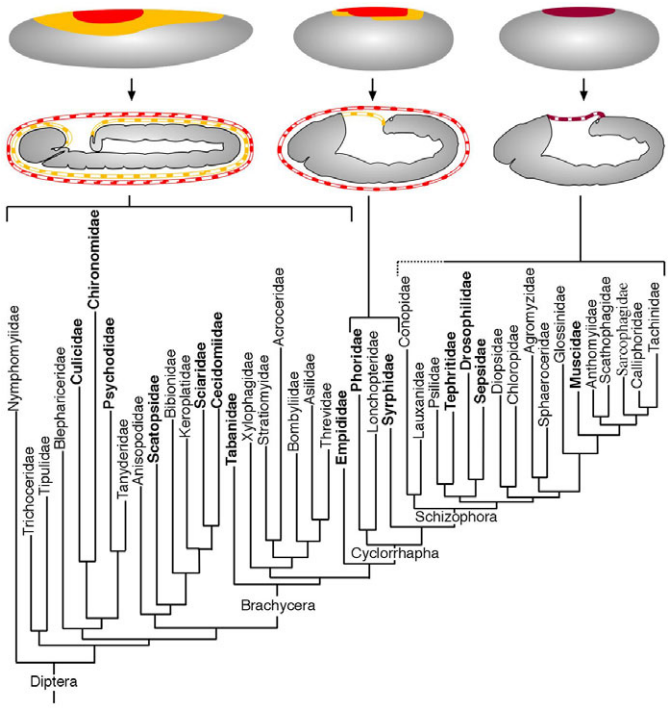

Fig. 1. Evolution of extra-embryonic tissue in flies (Diptera). Embryo sketches (anterior left, dorsal up) depicting the anlagen of the serosa (red) and amnion (orange) or amnioserosa (brown) as well as their topology upon differentiation in various fly families (taxa examined are in bold print) (reviewed by Rafiqi et al., 2011) are shown above the phylogeny of Diptera (Wiegmann et al., 2011).

staged embryos based on the position of the proctodeum. To quantify this position we projected the dorsalmost point of the proctodeum (the anterior-dorsal kink) onto the length axis of the embryo and determined its distance to the posterior pole relative to total egg length (proctodeum position in percent).

Image analysis

Fluorescent images for pMad profiles were taken using a Zeiss LSM510 confocal microscope. Microscope settings were adjusted to avoid saturation but were kept constant for embryos stained on the same day. Subsequently, the images were further analyzed using ImageJ. Profile plots of 'summary' *z*-projections (40 pixels thick) were obtained using the Plot Profile function; the data were exported into spreadsheets. The profiles were calibrated with reference to background fluorescence intensity, which was calculated by averaging intensities in the non-expressing lateral region of the embryo. To pool profile data of different embryos at the same developmental stage, amplitudes were adjusted by subtracting the average background value from all the values for a given embryo. Confocal imaging of NBT/BCIP precipitate was performed using a long-pass emission filter (LP 615, Zeiss); confocal imaging of VectorRed fluorescence was imaged with a Cy3 filter set.

Sequence analysis

Sequences were analyzed using the Geneious platform. Alignments were performed using ClustalW with a gap penalty of 3.0 and an extended gap penalty of 1.8 as recommended (Hall, 2001). Positions that were not conserved and represented in less than 20% of the sequences were removed from the alignment. Gene trees were generated using the maximum likelihood method in PHYML with the Jones-Taylor-Thornton substitution model and 500 bootstrap iterations (Guindon and Gascuel, 2003).

The sequences reported in this paper have been deposited in the GenBank database (accession numbers: *Mab-dpp*, JQ712977; *Mab-gbb*, JQ712978; *Mab-Sax*, JQ712979; *Mab-scw*, JQ712980; *Mab-sog*, JQ712981; and *Mab-tkv*, JQ712982).

RESULTS

Distinction of serosa and amnion in early *M. abdita* embryos

In *M. abdita*, serosa specification can be visualized by studying the expression of the *zen* homolog *Mab-zen* (Stauber et al., 1999). *Mab-zen* is activated at the beginning of cellularization and appears in a dorsal domain that spans ~16 cell diameters of the dorsoventral perimeter at 50% egg length (supplementary material Fig. S1). During early cellularization, the width of this domain narrows until it precisely coincides with the anlage of the serosa, which at 50% egg length is ~6-7 cell diameters in width (Fig. 2A,D). Specific markers for amniotic tissue have not been identified. Some markers, including *Mab-pnr*, *Mab-tup* and *Mab-doc*, that are activated in the dorsal blastoderm are later differentially repressed in the serosa, but they are not suitable to distinguish between amniotic and embryonic tissue because they are also expressed in the dorsal epidermis (Rafiqi et al., 2008; Rafiqi et al., 2010). Another marker, *Mab-hnt* (a homolog of *hindsight*, also known as *pebbled*), is expressed in the serosa and the amnion but not in the adjacent lateral epidermis of the germband (Rafiqi et al., 2010). To test whether earlier *Mab-hnt* expression occupies a broader domain than *Mab-zen* expression (serosa anlage), we performed double in situ hybridization experiments. Our method of detecting *Mab-zen* transcript (NBT/BCIP) precluded the detection of the *Mab-hnt* transcript in cells in which both genes are expressed owing to quenching of the *Mab-hnt* signal by NBT/BCIP, thereby highlighting *Mab-hnt*-positive cells in which *Mab-zen* is repressed. Both in the cellular blastoderm and during gastrulation, the dorsal expression domain of *Mab-hnt* was ~1-2 cell diameters broader than the expression domain of *Mab-zen* (Fig. 2A-D″). These observations show that *Mab-hnt* expression is broader than the serosa anlage.

To test whether the dorsal *Mab-hnt* expression domain overlaps with tissue that gives rise to the dorsal epidermis, we performed double in situ hybridizations with *Mab-eve*, a homolog of the pair-rule segmentation gene *even-skipped*, which is expressed in transverse stripes of the blastoderm (Bullock et al., 2004). Probes against *Mab-eve* and *Mab-zen* revealed that *Mab-eve* is gradually repressed in the serosa anlage (Fig. 3A-A‴). By the time the embryo entered gastrulation, a narrow gap had formed between the *Mab-zen* expression domain and the dorsalmost ends of the *Mab-eve* stripes (Fig. 3B-B‴). By contrast, the expression domains of *Mab-hnt* and *Mab-eve* abutted each other (Fig. 3C-D‴). We expected this result for gastrulating stages but not for blastoderm stages, given that *Mab-hnt* is activated in a broader domain than *Mab-zen* (Fig. 2A-B″). At blastoderm stages, *Mab-hnt* expression lateral to the *Mab-zen* domain might be too weak to be revealed by fluorescent in situ hybridization. Nevertheless, our observations suggest that in gastrulating embryos a rim of *Mab-hnt*-positive cells has formed around the serosa anlage, in which the expression of markers of the embryo proper is repressed. We suspect that these cells give rise to the amnion and propose that amnion specification occurs, at least laterally, after the specification of the serosa at the beginning of gastrulation.

BMP activity in early *M. abdita* embryos

Sequential patterning of the serosa and amnion raises the question of whether this process correlates with changes in the activity profile of BMPs. To address this question, we analyzed the distribution of pMad in *M. abdita* embryos at blastoderm and early gastrulation stages. The earliest embryos in which we could detect pMad were at the beginning of cellularization (Fig. 4A,A′). During

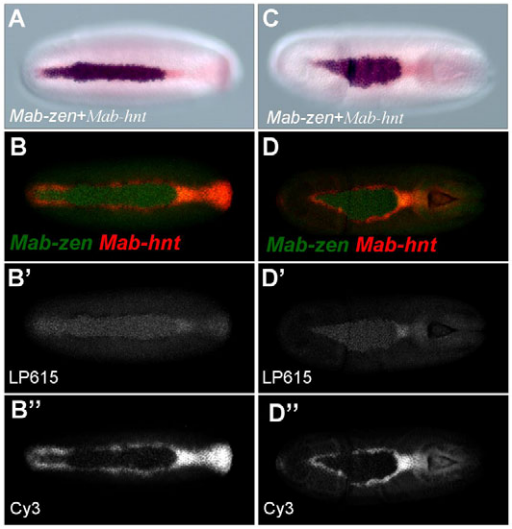

Fig. 2. Double in situ hybridizations for *Mab-zen* and *Mab-hnt*. (**A-D″**) Differential interference contrast (A,C) and confocal (B-B″,D-D″) images of *M. abdita* embryos (anterior left, dorsal view) at cellular blastoderm stage (A-B″) and gastrulation (C-D″). Transcripts were detected using alkaline phosphatase in the presence of NBT/BCIP (*Mab-zen*, dark blue in A,C) or VectorRed (*Mab-hnt*, red in A,C). Confocal images of NBT/BCIP precipitate were obtained using a long-pass emission filter (LP 615, Zeiss); fluorescence of VectorRed was detected in the Cy3 channel. B and D are merged false-color images of B′,B″ and D′,D″, respectively. Note that the fluorescent signal is quenched by NBT/BCIP.

blastoderm cellularization, we recorded a stronger signal with sharper boundaries, measuring at 50% egg length ~8-10 cell diameters in width (Fig. 4B,B′). The pMad domain varied in width along the anteroposterior axis and excluded the pole cells. During early gastrulation, the central portion of the pMad domain gradually broadened, concomitant with an apparent depletion of pMad levels in the center of the domain (Fig. 4C-F′). The lateral expansion of the pMad domain resulted primarily from pMad in additional cells, rather than from changes in cell shape.

In order to compare the lateral extent of the pMad domain with the serosa anlage, we double stained embryos for *Mab-zen* transcript (using NBT/BCIP) and pMad (using VectorRed). At the cellular blastoderm stage, the pMad domain was almost completely quenched along the dorsoventral perimeter, indicating that at this stage pMad levels are low along the lateral sides of the serosa anlage (Fig. 4G-G″). However, at early gastrulation stages the pMad domain was distinctly broader than the *Mab-zen* domain (Fig. 4H-H″). These observations suggest that, at the beginning of gastrulation, BMP activity increases in the lateral amnion.

Comparison of the BMP activity profiles between *M. abdita* and *D. melanogaster*

We next examined whether the difference in extra-embryonic tissue specification between *M. abdita* and *D. melanogaster* correlates with a difference in the BMP activity profiles of these two species. In *D. melanogaster*, our enzyme-based staining protocol for pMad produced a stronger signal than in *M. abdita*, and both before and after the onset of gastrulation we detected pMad in a slightly broader domain than *zen* (supplementary material Fig. S2). However, in these experiments potential saturation of the pMad staining might have obscured any temporal redistribution of pMad. To test whether *M. abdita* and *D. melanogaster* undergo comparable shifts in their respective pMad profiles during early gastrulation stages, we therefore examined the pMad levels of both species quantitatively using fluorophore-conjugated antibodies instead of enzyme-conjugated Fab fragments (antigen-binding fragments). In both species, the pMad profile of optical cross-sections (measured at 50% egg length) changed during early gastrulation, both in intensity and width. Specifically, we observed shallower and broader pMad profiles in gastrulating embryos than in late blastoderm embryos (Fig. 5A-G′; supplementary material Fig. S3). This transition occurred at slightly variable stages relative to our early gastrulation markers (mesoderm invagination, cephalic furrow formation, proctodeum position). To compare the profiles of multiple embryos within each species, we pooled similar pMad profiles and defined partially overlapping sequential developmental windows in which they occur (Fig. 5A′-G′). We then combined the average profiles of these groups in single graphs (Fig. 5H,I). This procedure revealed that during early gastrulation stages the pMad profile of *D. melanogaster* peaks at the dorsal midline, whereas the pMad profile of *M. abdita* peaks laterally (forming a saddle). These observations indicate a specific increase of pMad level in prospective amnion tissue of *M. abdita*, which is quantitatively distinct from the broadening of the pMad domain in *D. melanogaster* at comparable stages.

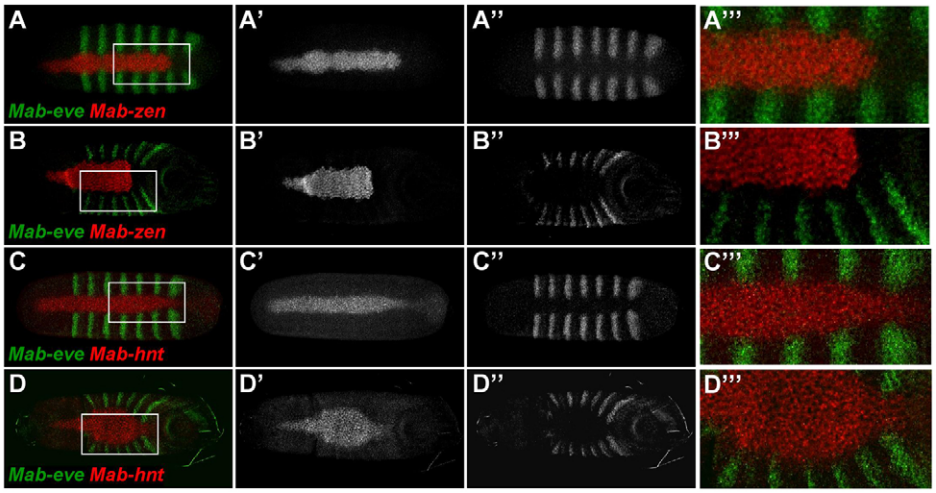

Fig. 3. Double in situ hybridizations for *Mab-eve* and *Mab-zen* or *Mab-hnt*. (**A-D‴**) *Mab-eve* and *Mab-zen* (A-B‴) or *Mab-eve* and *Mab-hnt* (C-D‴) expression at the cellular blastoderm stage (A-A‴,C-C‴) and during early gastrulation (B-B‴,D-D‴). *Mab-eve* was detected using Cy3 (green); *Mab-zen* and *Mab-hnt* were detected with Alexa Fluor 488 (red). Note the gap between the dorsal edges of the *Mab-eve* stripes and the *Mab-zen* domain, in particular at the later stage (B). By contrast, the *Mab-eve* stripes abut the *Mab-hnt* domain of gastrulating embryos (D). Dorsal view, anterior to the left. Boxed regions in A-D are enlarged in A‴-D‴.

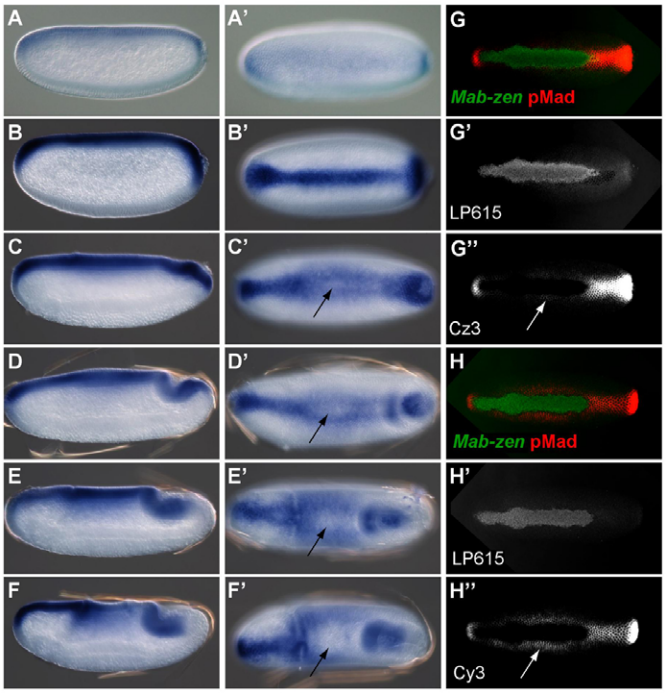

Fig. 4. pMad and *Mab-zen* transcript in *M. abdita*. (**A-F'**) pMad domains at consecutive blastoderm (A-B′) and early gastrulation (C-F′) stages. Note the reduced mid-central pMad levels in gastrulating embryos (black arrows). Lateral and dorsal view with anterior to the left. (**G-H″**) pMad and *Mab-zen* transcript shortly before (G-G″) and shortly after (H-H″) the onset of gastrulation. *Mab-zen* transcript was detected using NBT/BCIP (LP615 channel) and pMad using VectorRed (Cy3 channel), which is quenched in the presence of NBT/BCIP precipitate. Note the increased pMad signal lateral to the *Mab-zen* domain after the beginning of gastrulation (white arrows). Dorsal view with anterior to the left.

Expression of BMP signaling components in the *M. abdita* embryo

To test whether BMP signaling in the prospective serosa and amnion involves the same set of BMP signaling components, we cloned *M. abdita* homologs of the BMP ligand genes *dpp* (*Mab-dpp*), *scw* (*Mab-scw*) and *gbb* (*Mab-gbb*) (supplementary material Fig. S4), the BMP receptor genes *sax* (*Mab-sax*) and *tkv* (*Mab-tkv*) (supplementary material Fig. S5), and the BMP antagonist gene *sog* (*Mab-sog*) (supplementary material Fig. S6). In this section we document their specific expression patterns as revealed by whole-mount in situ hybridization and show that all these genes are expressed during early development in *M. abdita*.

Mab-dpp expression was detected on the dorsal side of the late blastoderm and gastrula (Fig. 6A-D′). After gastrulation, *Mab-dpp* expression was most prominent in a band of dorsal epidermis but not in its leading edge (Fig. 6E). However, after stomodeum formation [corresponding roughly to stage 10 in *D. melanogaster* (Campos-Ortega and Hartenstein, 1997)], a prominent stripe of *Mab-dpp* expression was observed ~1 cell diameter away from the leading edge of the epidermis. In part, the transcripts forming this expression domain seemed to belong to leading edge cells but their subcellular localization was opposite to the side of the amnion (Fig. 6F). We also noticed expression in more lateral epidermal and presumably mesodermal cells of the trunk segments, and in parts of the gnathal segments and clypeolabrum. After pharynx differentiation (corresponding roughly to stage 11 in *D. melanogaster*) a new, presumably mesodermal domain was observed in the first and second abdominal segments (Fig. 6G). *Mab-scw* expression was nearly ubiquitous, but weak and only detected during blastoderm stages (Fig. 6H-J). *Mab-gbb* was expressed in a broad dorsal domain of the blastoderm but not at the poles (Fig. 6K,K′). During gastrulation, *Mab-gbb* expression was strong in the serosa and amnion (Fig. 6L), but at the end of gastrulation *Mab-gbb* expression was stronger in the amnion than in the serosa (Fig. 6M). After stomodeum formation, *Mab-gbb* was expressed in the leading edge of the epidermis, in more lateral portions of the trunk and head epidermis, and in a cellular band of the mesoderm (Fig. 6N,N′). In summary, all three BMP ligand genes were expressed in the blastoderm but *Mab-scw* was downregulated prior to gastrulation and only *Mab-dpp* and *Mab-gbb* were expressed in older embryos.

Mab-sax was ubiquitously expressed until early gastrulation. Subsequently, the transcript was predominantly detected in the mesoderm (Fig. 7A-C). *Mab-tkv* transcript was also detected ubiquitously until gastrulation. During gastrulation, *Mab-tkv* expression shifted to the ventral side, including the mesoderm (Fig. 7D-F). *Mab-sog* expression started during the cellular blastoderm stage as a pair of broad lateral stripes (Fig. 7G,G′). During mesoderm invagination, the *Mab-sog* expression domains converged towards the ventral midline (Fig. 7H,H′). At this stage, *Mab-sog* expression was also detected in a number of cells in the gap between the *Mab-sog* stripes. By the time the embryo started germ band extension, the two stripes were close to each other as a result of ventral mesoderm invagination but, with the exception of a row of *Mab-sog*-positive cells at the ventral midline, a small gap remained throughout gastrulation (Fig. 7I,I′). In the head region, the stripes extended dorsally.

Role of specific BMP signaling components in serosa and amnion specification

To test whether serosa and amnion specification require BMP signaling and depend on the same set of BMP signaling components, we repressed *Mab-dpp*, *Mab-scw*, *Mab-gbb*, *Mab-sax*, *Mab-tkv* or *Mab-sog* by RNAi and tested for suppression of *Mab-zen* and *Mab-hnt* activation and for ectopic dorsal expression of *Mab-eve*. All components of the BMP pathway that we tested in this way affected dorsal patterning but did so with varying efficiency (Fig. 8; Fig. 9A-L). RNAi against *Mab-dpp* most efficiently suppressed the dorsal expression of *Mab-zen* (27/27) and *Mab-hnt* (25/25) and prevented the dorsal repression of *Mab-eve* (45/55) (Fig. 9A-F). RNAi against *Mab-scw* or *Mab-gbb* caused suppression of *Mab-zen* (20/41 or 29/77) and *Mab-hnt* (9/51 or 27/77) activation less frequently and almost never interfered with the dorsal repression of *Mab-eve* stripes (1/50 or 4/82). Double RNAi against *Mab-scw* and *Mab-gbb* proved slightly more efficient (26/40 for *Mab-zen*; 13/40 for *Mab-hnt*; 5/23 for *Mab-eve*) but was still much less efficient than RNAi against *Mab-dpp*.

Among the receptors, RNAi against *Mab-sax* suppressed the activation of *Mab-zen* (24/25) and *Mab-hnt* (23/31) and caused ectopic dorsal expression of *Mab-eve* (21/29) in most embryos (Fig. 9G-I), whereas *Mab-tkv* RNAi was less efficient in suppressing the activation of *Mab-zen* (26/40) and *Mab-hnt* (13/39) and almost never interfered with the dorsal repression of *Mab-eve* stripes (1/32). *Mab-sog* RNAi resulted in suppression or in reduction and broadening of *Mab-zen* (57/57) and *Mab-hnt* (44/44) activation (Fig. 9J,K) and interfered with the dorsal repression of *Mab-eve* (18/26) (Fig. 9L).

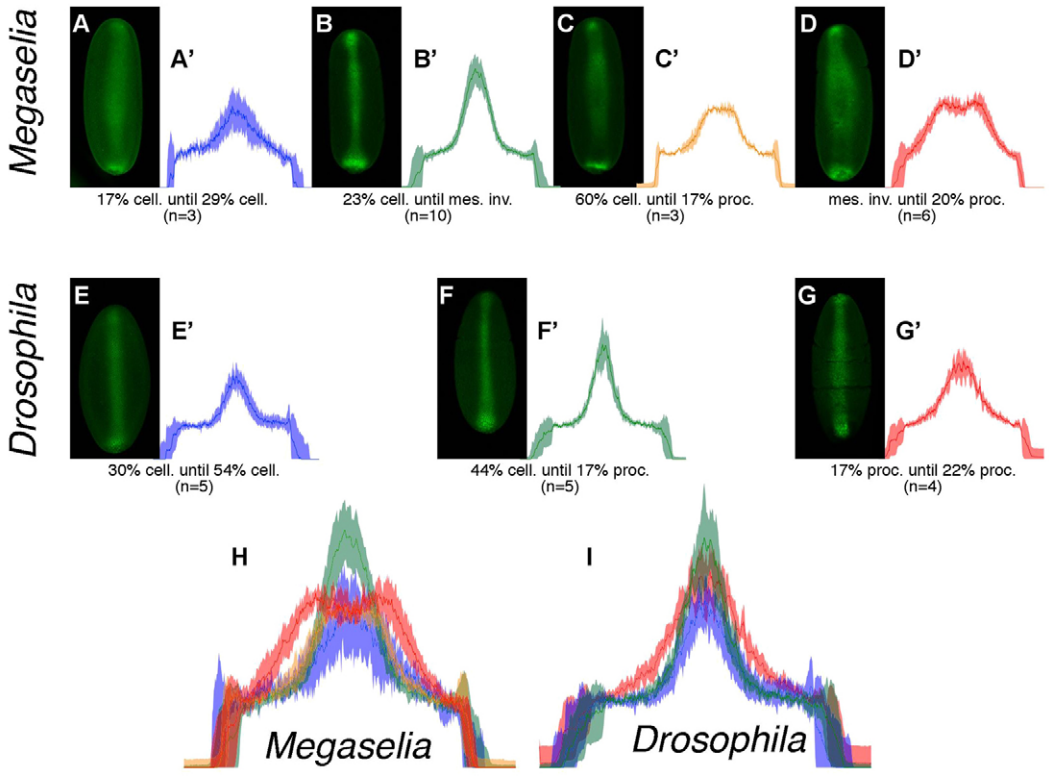

Fig. 5. Distinct pMad dynamics in *M. abdita* and *D. melanogaster*. (**A-G'**) pMad in *M. abdita* (A-D) and *D. melanogaster* (E-G) embryos (dorsal view, anterior up) at consecutive developmental stages alongside pooled cross-sectional pMad profiles taken at 50% egg length (A′-G′). pMad was detected using Cy3-conjugated antibodies. The profiles show average pMad levels (dark line) ± s.d. (paler color). The developmental windows from which profiles were pooled are indicated. % cell., percentage blastoderm cellularization; mes. inv., mesoderm invagination; % proc., position of proctodeum relative to egg length. (**H**,**I**) Combined pMad profile groups of *M. abdita* (H) and *D. melanogaster* (I).

Evidence for a positive-feedback loop in BMP signaling

In *D. melanogaster*, a positive-feedback loop refines BMP activity along the dorsal midline (Wang and Ferguson, 2005). This feedback response transforms the initially broad and shallow gradient of BMP activity in blastoderm embryos into a much narrower and steeper gradient. In *D. melanogaster*, the mechanism was discovered by monitoring extracellular BMP-receptor interactions and intracellular pMad in blastoderm embryos that had been injected with mRNA of constitutively active Tkv (*tkv-a*). Tkv-a induces a correlated wave front of BMP-receptor interactions and intracellular pMad, which is accompanied by a decrease of receptor-bound ligand and pMad in adjacent cells. None of these effects is observed following injection of wild-type *tkv* mRNA, indicating that a positive-feedback mechanism is crucial to achieve the local boost in BMP activity (Wang and Ferguson, 2005).

Positive feedback of BMP signaling could be essential for the dynamic changes in the pMad domain that occur during blastoderm and gastrulation stages (see Discussion). To test whether such a feedback loop exists in early *M. abdita* embryos, we injected *tkv-a* mRNA into *M. abdita* embryos at the syncytial blastoderm stage and monitored its effect on the expression of *Mab-zen* and *Mab-hnt* (we used these markers instead of pMad because of background problems with the detection of pMad in the injected embryos). The injection of *tkv-a* mRNA consistently induced ectopic expression of *Mab-zen* (40/44) and *Mab-hnt* (34/35) anywhere along the dorsoventral axis, and often caused a reduction of endogenous expression, especially in the immediate vicinity of induced dorsal expression domains (Fig. 9M,N). None of these effects was observed when injecting *tkv* mRNA and staining for *Mab-zen* (n=20) or *Mab-hnt* (n=31). Conversely, injection of *Xenopus noggin* mRNA, which has been shown to repress BMP signaling in *D. melanogaster* (Holley et al., 1996), caused a reduction of *Mab-zen* (28/48) and *Mab-hnt* (12/40) expression in *M. abdita* (Fig. 9O). From these experiments, we conclude that BMP signaling in early *M. abdita* embryos is subject to a positive-feedback loop that refines the dorsal expression domains of *Mab-zen* and *Mab-hnt*.

DISCUSSION

The role of BMP signaling in serosa and amnion specification in *M. abdita*

Flies experienced an evolutionary reduction of extra-embryonic tissue types from two to one, which must have been accompanied by changes in dorsal embryonic patterning. Here we have examined BMP signaling, a key regulator of dorsal patterning, in early embryos of *M. abdita*, a dipteran fly with distinct serosal and amniotic tissues and a close outgroup of schizophoran flies that develop a single amnioserosa. We found that in *M. abdita*, serosa and amnion patterning is dependent on a range of BMP signaling components. Furthermore, we identified a conspicuous difference in the dynamic BMP activity profile between *M. abdita* and *D. melanogaster*, which coincides in time and space with early signs of lateral amnion specification in gastrulating *M. abdita* embryos. Here we discuss our findings in the light of potential models of serosa and amnion specification and propose a synthesis of the available data.

Previously, it has been proposed that serosal and amniotic tissue types are specified by distinct threshold responses to a BMP activity gradient, which peaks along the dorsal midline of the blastoderm (Goltsev et al., 2007). Consistent with this idea, we found in *M. abdita* blastoderm embryos that pMad levels form a gradient that peaks at the dorsal midline, and that *Mab-hnt*, a marker of prospective serosa and amnion tissues, is activated in a broader domain than *Mab-zen*. However, although amnion specification might begin at the blastoderm stage, the distinction of lateral amnion cells from embryonic cells is still unclear at this stage as indicated by the confluent expression

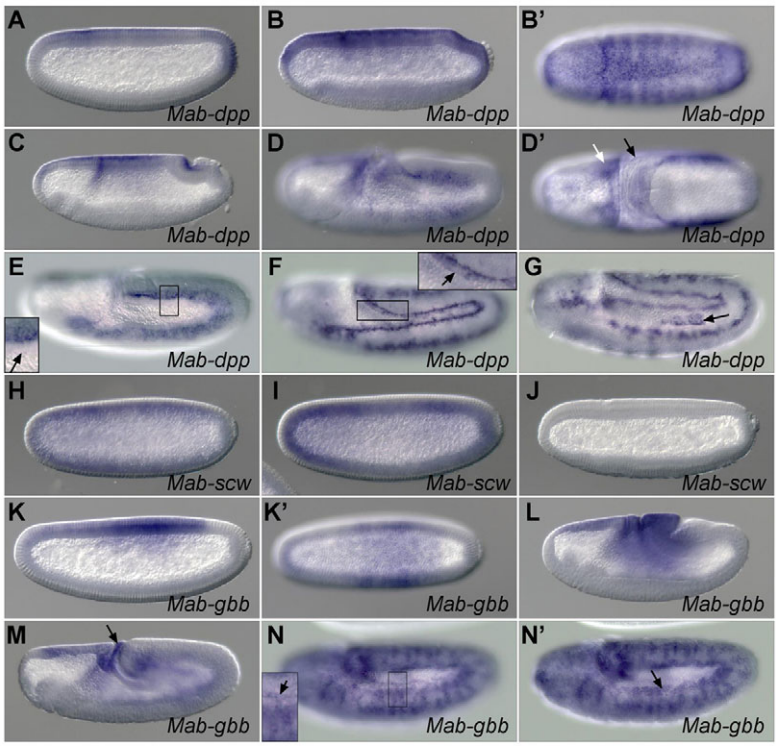

Fig. 6. Expression of *Mab-dpp*, *Mab-scw* and *Mab-gbb*. (**A-G**) *Mab-dpp* in situ hybridizations at the stage of late blastoderm cellularization (A), consecutive stages of gastrulation (B-D′), and extended germband stages before (E) and after (F) stomodeum formation, and after pharynx formation (G). Arrows mark expression in the extra-embryonic tissue (black arrow in D′) and in the optic lobes (white arrow in D′), the leading edge of the epidermis (insets in E,F), and a presumably mesodermal expression domain in the first and second abdominal segments (G). (**H-J**) *Mab-scw* in situ hybridizations at the syncytial blastoderm stage (H), at the stage of blastoderm cellularization (I) and at the end of the cellular blastoderm stage (J). (**K-N′**) *Mab-gbb* in situ hybridizations during blastoderm cellularization (K,K′), consecutive gastrulation stages (L,M) and after stomodeum formation (N,N′). Arrows mark amniotic expression (M), the leading edge of the dorsal epidermis (inset in N) and a band of mesodermal expression (N′). Dorsal view (B′,D′,K′) or in lateral view with the dorsal side up; anterior is left.

domains of the embryonic marker *Mab-eve* and the serosa marker *Mab-zen*. We therefore believe that lateral amnion specification is delayed until early gastrulation, when the *Mab-eve* stripes have receded from the *Mab-zen* domain and now abut the dorsal *Mab-hnt* expression domain. This observation suggests that the specification of serosa tissue and that of the amnion occur, at least in part, at different time points: serosa specification at the cellular blastoderm stage and (lateral) amnion specification at the beginning of gastrulation.

Amnion patterning during early gastrulation correlates with a quantitative shift of the peak pMad level away from the serosa towards the region that gives rise to the amnion (Fig. 4G,H). In early gastrulation stages of *D. melanogaster*, this change in the pMad profile appeared attenuated and was quantitatively clearly distinct from that in *M. abdita* (Fig. 5H,I). The redistribution of pMad during early gastrulation might be important for specifying the amnion in *M. abdita*.

At present, it is unclear which factor or factors cause the dynamic change of the pMad profile during early gastrulation in *M. abdita*. The broadening of the pMad domain at this stage could be dependent on a target of the Toll signaling pathway, which presumably functions as a conserved dorsoventral pattern organizer on the ventral side (Lynch and Roth, 2011), or a factor downstream of BMP signaling. Alternatively, the positive-feedback loop of BMP signaling, for which we obtained evidence in *M. abdita*, could explain the dynamics of BMP activity both in the blastoderm and during early gastrulation. In the blastoderm, analogous to the role of positive feedback of BMP signaling in *D. melanogaster*, this mechanism might refine and enhance BMP signaling in the *M. abdita* embryo and thereby influence the expression boundaries of target genes such as *Mab-zen*, *Mab-hnt* and *Mab-eve*. At the beginning of gastrulation, positive feedback could drive the dorsocentral depression and lateral shift of BMP activity. In line with this idea, experimental

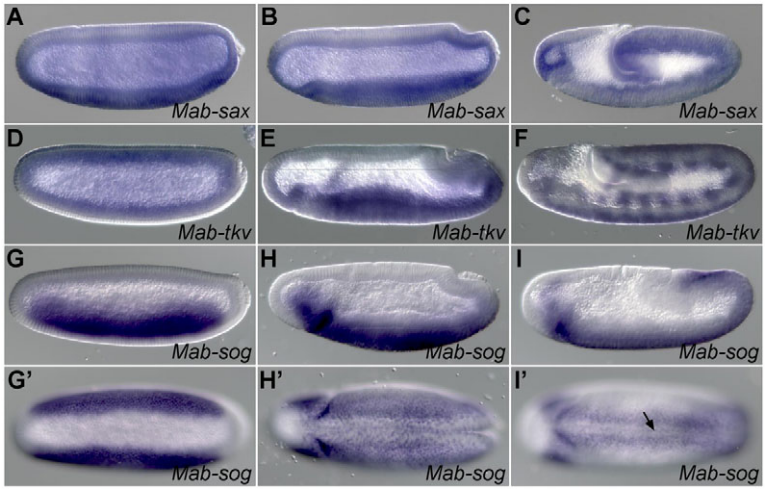

Fig. 7. Expression of *Mab-sax*, *Mab-tkv* and *Mab-sog*. (**A-C**) *Mab-sax* in situ hybridizations at the cellular blastoderm stage (A) and consecutive gastrulation stages (B,C). (**D-F**) *Mab-tkv* in situ hybridizations at the syncytial blastoderm stage (D), gastrulation stage (E) and the extended germband stage after stomodeum formation (F). (**G-I′**) *Mab-sog* in situ hybridizations at the syncytial blastoderm stage (G,G′) and consecutive gastrulation stages (H-I′). Lateral view with dorsal side up (A-I) or ventral view (G′,H′,I′); anterior is left. The arrow (I′) points to *Mab-sog* expression at the ventral midline splitting the mid-ventral gap of low *Mab-sog* expression into left and right halves.

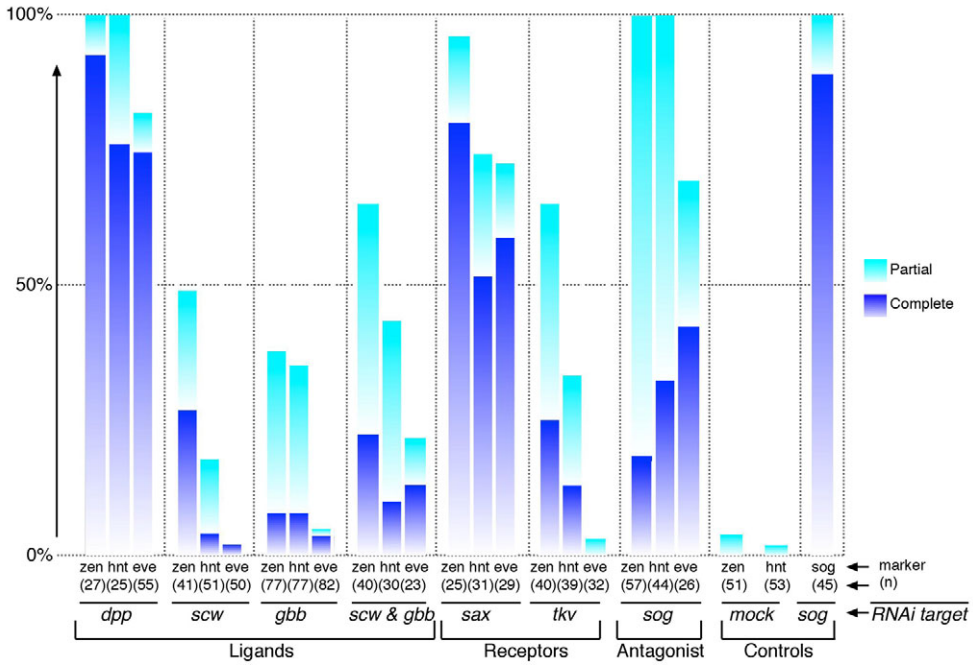

Fig. 8. Perturbation of extra-embryonic patterning in various RNAi backgrounds. Following RNAi against specific BMP signaling components, *M. abdita* embryos were scored for dorsal expression of *Mab-zen*, *Mab-hnt* or *Mab-eve*. Bars indicate the percentage of embryos in which *Mab-zen* or *Mab-hnt* expression was missing (dark blue) or reduced (light blue), or in which *Mab-eve* stripes had all failed (dark blue) or failed in part (light blue) to split along the dorsal midline.

perturbation of BMP activity in early *D. melanogaster* embryos and mathematical modeling suggest that, in the presence of hyperactive positive feedback, an imbalance of receptor-bound BMP and Sog-mediated transport can change the directionality of extracellular BMP flux to the extent that a single domain of high BMP activity splits into two distinct peaks (Umulis et al., 2010). In wild-type *M. abdita* embryos, the balance of receptor-bound BMPs and Sog-mediated transport could be such that, under the influence of continuous positive BMP signaling feedback, the center of BMP activity shifts towards the amnion. Accordingly, suppression of positive BMP signaling during blastoderm stages should affect both serosa and amnion specification, whereas suppression of this feedback loop at the beginning of gastrulation would perturb amnion development. It should be possible to test this hypothesis once the molecular details of the positive-feedback loop are better understood.

In summary, our findings are consistent with a mixed model of serosa and amnion specification involving threshold responses to a BMP gradient, autoregulation of the BMP profile and differential response to high BMP activity over time (Fig. 10).

Evolution of BMP signaling in the early fly embryo

Our interpretation of the dynamic change of BMP activity during early gastrulation as an important factor in amnion specification raises the question of whether the increase of BMP activity in prospective amnion of early gastrula stages is conserved in other species. Functional data on extra-embryonic tissue specification in

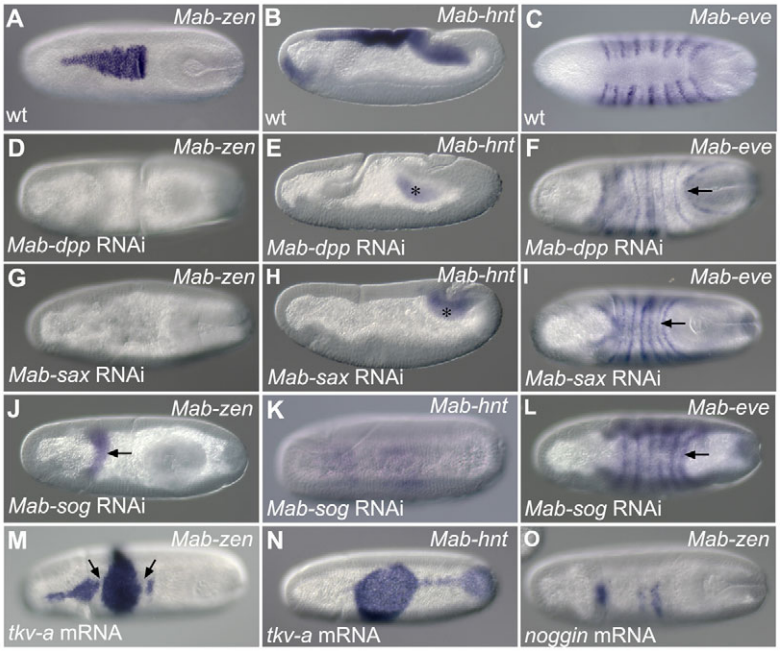

Fig. 9. Representative expression phenotypes following perturbation of BMP signaling. (**A-C**) Expression of *Mab-zen* (A), *Mab-hnt* (B) and *Mab-eve* (C) in wild-type embryos at early gastrulation stages. (**D-L**) Expression of the same genes following RNAi against *Mab-dpp* (D-F), *Mab-sax* (G-I) or *Mab-sog* (J-L). Proctodeal expression of *Mab-hnt* (asterisks in E,H), circumferential *Mab-eve* stripes (arrows in F,I,L), and the broadened residual expression domain of *Mab-zen* (arrow in J) are indicated. (**M**,**N**) Expression of *Mab-zen* (M) or *Mab-hnt* (N) following injection of *tkv-a* mRNA. Note the repression of endogenous expression near ectopically induced expression (arrows in M). (**O**) Expression of *Mab-zen* following injection of *Xenopus noggin* mRNA. Anterior is to the left in dorsal (A,C,D,F,G,I-O) or lateral (B,E,H) view.

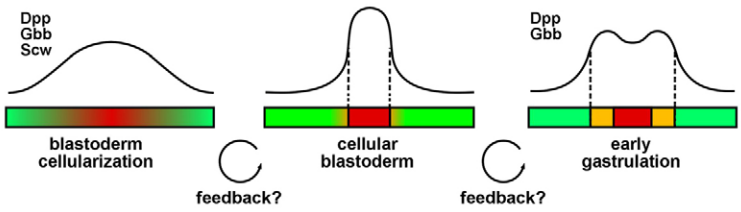

Fig. 10. Model for BMP-dependent serosa and amnion specification in *M. abdita*. Consecutive BMP activity profiles (continuous lines) are shown above sketches of the developing dorsal fate map illustrating prospective serosa (red), amnion (orange) and embryonic ectoderm (green). The midpoint of each fate map represents the dorsalmost position. Dashed vertical lines indicate hypothetical threshold responses to BMP activity. BMP ligands are provided by *Mab-dpp*, *Mab-gbb* and *Mab-scw*, but at the beginning of gastrulation *Mab-scw* is no longer expressed.

the beetle *Tribolium castaneum* provide material for an outgroup comparison, which allows us to assess the directionality of the evolutionary change that we observe between cyclorrhaphan flies. In *T. castaneum*, the serosa is a derivative of anterior and dorsal blastoderm (Falciani et al., 1996) and is dependent on two signaling pathways: Torso (Tor) and BMP. Tor is a MAP kinase signaling pathway (Li, 2005), which in cyclorrhaphan flies controls the development of terminal embryonic structures (Sprenger and Nüsslein-Volhard, 1993; Lemke et al., 2010). In *T. castaneum*, downregulation of the Tor pathway by RNAi causes a severe reduction of the serosa anlage (Schoppmeier and Schröder, 2005), whereas downregulation of the BMP pathway by RNAi against *T. castaneum dpp* (*Tc-dpp*) only suppresses a dorsal portion of the serosa anlage (van der Zee et al., 2006). Whereas *Tc-dpp* appears to control serosa specification only in part, its role in amnion specification appears to be crucial. *Tc-dpp* RNAi suppresses the expression of *Tc-pnr*, an early amnion marker, which indicates that *Tc-dpp* is required for amnion specification. The BMP activity profile of early *T. castaneum* embryos is consistent with its predominant role in the amnion. Initially, *T. castaneum* pMad accumulates along the whole dorsal side of the blastoderm embryo and tapers off laterally, but with the beginning of gastrulation, peak levels of pMad shift to the amnion (van der Zee et al., 2006; Nunes da Fonseca et al., 2008). The accumulation of pMad at the onset of gastrulation in the prospective amnion in *T. castaneum* is reminiscent of the shifting pMad peak levels in *M. abdita* embryos during early gastrulation. The apparent conservation of this feature in distantly related insects with serosal and amniotic tissues but distinct blastoderm fate maps suggests that BMP-dependent amnion specification requires BMP signaling in the prospective amnion at the beginning of gastrulation. Therefore, BMP-dependent amnion specification could be an ancient evolutionary heritage of insects, whereas the essential requirement of high BMP levels for serosa specification might have evolved in dipterans.

BMP signaling and the evolution of *sog* expression

The blastodermal pMad domain is much broader in the mosquito *A. gambiae* than in *D. melanogaster* or in *M. abdita*. The broad pMad domain of *A. gambiae* correlates with ventral (mesodermal) *sog* expression, which we found to be conserved in the harlequin fly *Chironomus riparius* (Chironomidae), a distant relative of *A. gambiae* (supplementary material Fig. S7A-B′). Mesodermal *sog* expression has also been reported for *T. castaneum* (van der Zee et al., 2006). By contrast, the comparatively narrow pMad domains of *D. melanogaster* (supplementary material Fig. S7C-E′) and *M. abdita* (Fig. 7G,G′) correlate with predominantly lateral (neuroectodermal) *sog* expression. This correlation is also conserved in *Episyrphus balteatus* (Syrphidae), another cyclorrhaphan fly with serosal and amniotic tissue (supplementary material Fig. S7G-I′). In summary, a shift in *sog* expression from ventral to lateral blastoderm might have been an important factor in narrowing the early embryonic activity range of BMP signaling in dipteran evolution, as proposed previously (Goltsev et al., 2007). However, the phenotypic consequences of shifting the center of *sog* expression from the mesoderm anlage to the neurogenic ectoderm are still unclear. Our data suggest that neuroectodermal *sog* expression evolved in the stem lineage of cyclorrhaphan flies possibly in conjunction with the evolutionary transition form ventral to dorsal amnion closure (Fig. 1).

Acknowledgements
We thank Caroline Albertin for cloning *Mab-sax and Mab-tkv* genes in the course of a laboratory rotation project; Ed Laufer for providing pMad antibody; Johannes Jaeger (Barcelona, Spain) for sharing *M. abdita* transcriptome data; our colleagues Chip Ferguson and Jackie Gavin-Smyth for discussions; Jackie Gavin-Smyth for kindly training C.W.K. at the confocal microscope; and Ehab Abouheif (Montreal, Canada) and his laboratory members for feedback on the manuscript.

Funding
This project was supported by the National Science Foundation [grant 1121211] and institutional funds of the University of Chicago to U.S.-O.

Competing interests statement
The authors declare no competing financial interests.

Supplementary material
Supplementary material available online at
http://dev.biologists.org/lookup/suppl/doi:10.1242/dev.083873/-/DC1

References

Arora, K. and Nüsslein-Volhard, C. (1992). Altered mitotic domains reveal fate map changes in *Drosophila* embryos mutant for zygotic dorsoventral patterning genes. *Development* **114**, 1003-1024.
Arora, K., Levine, M. S. and O'Connor, M. B. (1994). The *screw* gene encodes a ubiquitously expressed member of the TGF-beta family required for specification of dorsal cell fates in the *Drosophila* embryo. *Genes Dev.* **8**, 2588-2601.
Ashe, H. L. and Levine, M. (1999). Local inhibition and long-range enhancement of Dpp signal transduction by Sog. *Nature* **398**, 427-431.
Biehs, B., François, V. and Bier, E. (1996). The *Drosophila short gastrulation* gene prevents Dpp from autoactivating and suppressing neurogenesis in the neuroectoderm. *Genes Dev.* **10**, 2922-2934.
Bullock, S. L., Stauber, M., Prell, A., Hughes, J. R., Ish-Horowicz, D. and Schmidt-Ott, U. (2004). Differential cytoplasmic mRNA localisation adjusts pair-rule transcription factor activity to cytoarchitecture in dipteran evolution. *Development* **131**, 4251-4261.
Campos-Ortega, J. A. and Hartenstein, V. (1997). *The Embryonic Development of Drosophila melanogaster*. Berlin: Springer-Verlag.
Decotto, E. and Ferguson, E. L. (2001). A positive role for Short gastrulation in modulating BMP signaling during dorsoventral patterning in the *Drosophila* embryo. *Development* **128**, 3831-3841.

Eldar, A., Dorfman, R., Weiss, D., Ashe, H., Shilo, B. Z. and Barkai, N. (2002). Robustness of the BMP morphogen gradient in *Drosophila* embryonic patterning. *Nature* **419**, 304-308.
Falciani, F., Hausdorf, B., Schröder, R., Akam, M., Tautz, D., Denell, R. and Brown, S. (1996). Class 3 Hox genes in insects and the origin of *zen*. *Proc. Natl. Acad. Sci. USA* **93**, 8479-8484.
Ferguson, E. L. and Anderson, K. V. (1992a). Decapentaplegic acts as a morphogen to organize dorsal-ventral pattern in the *Drosophila* embryo. *Cell* **71**, 451-461.
Ferguson, E. L. and Anderson, K. V. (1992b). Localized enhancement and repression of the activity of the TGF-beta family member, *decapentaplegic*, is necessary for dorsal-ventral pattern formation in the *Drosophila* embryo. *Development* **114**, 583-597.
Francois, V., Solloway, M., O'Neill, J. W., Emery, J. and Bier, E. (1994). Dorsal-ventral patterning of the Drosophila embryo depends on a putative negative growth factor encoded by the *short gastrulation* gene. *Genes Dev.* **8**, 2602-2616.
Fritsch, C., Lanfear, R. and Ray, R. P. (2010). Rapid evolution of a novel signalling mechanism by concerted duplication and divergence of a BMP ligand and its extracellular modulators. *Dev. Genes Evol.* **220**, 235-250.
Goltsev, Y., Fuse, N., Frasch, M., Zinzen, R. P., Lanzaro, G. and Levine, M. (2007). Evolution of the dorsal-ventral patterning network in the mosquito, *Anopheles gambiae*. *Development* **134**, 2415-2424.
Goltsev, Y., Rezende, G. L., Vranizan, K., Lanzaro, G., Valle, D. and Levine, M. (2009). Developmental and evolutionary basis for drought tolerance of the *Anopheles gambiae* embryo. *Dev. Biol.* **330**, 462-470.
Guindon, S. and Gascuel, O. (2003). A simple, fast, and accurate algorithm to estimate large phylogenies by maximum likelihood. *Syst. Biol.* **52**, 696-704.
Hall, B. G. (2001). *Phylogenetic Trees Made Easy: a How-to Manual for Molecular Biologists*. Sunderland, MA: Sinauer Associates.
Holley, S. A., Neul, J. L., Attisano, L., Wrana, J. L., Sasai, Y., O'Connor, M. B., De Robertis, E. M. and Ferguson, E. L. (1996). The *Xenopus* dorsalizing factor noggin ventralizes *Drosophila* embryos by preventing DPP from activating its receptor. *Cell* **86**, 607-617.
Kosman, D., Mizutani, C. M., Lemons, D., Cox, W. G., McGinnis, W. and Bier, E. (2004). Multiplex detection of RNA expression in *Drosophila* embryos. *Science* **305**, 846.
Lemke, S., Busch, S. E., Antonopoulos, D. A., Meyer, F., Domanus, M. H. and Schmidt-Ott, U. (2010). Maternal activation of gap genes in the hover fly *Episyrphus*. *Development* **137**, 1709-1719.
Lemke, S., Antonopoulos, D. A., Meyer, F., Domanus, M. H. and Schmidt-Ott, U. (2011). BMP signaling components in embryonic transcriptomes of the hover fly *Episyrphus balteatus* (Syrphidae). *BMC Genomics* **12**, 278.
Li, W. X. (2005). Functions and mechanisms of receptor tyrosine kinase Torso signaling: lessons from *Drosophila* embryonic terminal development. *Dev. Dyn.* **232**, 656-672.
Liang, H. L., Nien, C. Y., Liu, H. Y., Metzstein, M. M., Kirov, N. and Rushlow, C. (2008). The zinc-finger protein Zelda is a key activator of the early zygotic genome in *Drosophila*. *Nature* **456**, 400-403.
Lynch, J. A. and Roth, S. (2011). The evolution of dorsal-ventral patterning mechanisms in insects. *Genes Dev.* **25**, 107-118.
Marqués, G., Musacchio, M., Shimell, M. J., Wünnenberg-Stapleton, K., Cho, K. W. and O'Connor, M. B. (1997). Production of a DPP activity gradient in the early *Drosophila* embryo through the opposing actions of the SOG and TLD proteins. *Cell* **91**, 417-426.
Mizutani, C. M., Meyer, N., Roelink, H. and Bier, E. (2006). Threshold-dependent BMP-mediated repression: a model for a conserved mechanism that patterns the neuroectoderm. *PLoS Biol.* **4**, e313.
Neul, J. L. and Ferguson, E. L. (1998). Spatially restricted activation of the SAX receptor by SCW modulates DPP/TKV signaling in *Drosophila* dorsal-ventral patterning. *Cell* **95**, 483-494.
Niehrs, C. (2010). On growth and form: a Cartesian coordinate system of Wnt and BMP signaling specifies bilaterian body axes. *Development* **137**, 845-857.
Nunes da Fonseca, R., von Levetzow, C., Kalscheuer, P., Basal, A., van der Zee, M. and Roth, S. (2008). Self-regulatory circuits in dorsoventral axis formation of the short-germ beetle *Tribolium castaneum*. *Dev. Cell* **14**, 605-615.
O'Connor, M. B., Umulis, D., Othmer, H. G. and Blair, S. S. (2006). Shaping BMP morphogen gradients in the *Drosophila* embryo and pupal wing. *Development* **133**, 183-193.
Padgett, R. W., St Johnston, R. D. and Gelbart, W. M. (1987). A transcript from a *Drosophila* pattern gene predicts a protein homologous to the transforming growth factor-beta family. *Nature* **325**, 81-84.
Rafiqi, A. M., Lemke, S., Ferguson, S., Stauber, M. and Schmidt-Ott, U. (2008). Evolutionary origin of the amnioserosa in cyclorrhaphan flies correlates with spatial and temporal expression changes of *zen*. *Proc. Natl. Acad. Sci. USA* **105**, 234-239.
Rafiqi, A. M., Lemke, S. and Schmidt-Ott, U. (2010). Postgastrular *zen* expression is required to develop distinct amniotic and serosal epithelia in the scuttle fly *Megaselia*. *Dev. Biol.* **341**, 282-290.
Rafiqi, A. M., Lemke, S. and Schmidt-Ott, U. (2011). The scuttle fly *Megaselia abdita* (Phoridae): a link between Drosophila and Mosquito development. *Cold Spring Harb. Protoc.* **2011**, pdb emo143.
Ray, R. P., Arora, K., Nüsslein-Volhard, C. and Gelbart, W. M. (1991). The control of cell fate along the dorsal-ventral axis of the *Drosophila* embryo. *Development* **113**, 35-54.
Rothwell, W. F. and Sullivan, W. (2000). Fluorescent analysis of *Drosophila* embryos. In *Drosophila Protocols* (ed. W. Sullivan, M. Ashburner and R. S. Hawley). Cold Spring Harbor, NY: Cold Spring Harbor Laboratory Press.
Rushlow, C., Colosimo, P. F., Lin, M. C., Xu, M. and Kirov, N. (2001). Transcriptional regulation of the *Drosophila* gene *zen* by competing Smad and Brinker inputs. *Genes Dev.* **15**, 340-351.
Schmidt-Ott, U., Rafiqi, A. M. and Lemke, S. (2010). *Hox3/zen* and the evolution of extraembryonic epithelia in insects. *Adv. Exp. Med. Biol.* **689**, 133-144.
Schneider, C. A., Rasband, W. S. and Eliceiri, K. W. (2012). NIH Image to ImageJ: 25 years of image analysis. *Nat. Methods* **9**, 671-675.
Schoppmeier, M. and Schröder, R. (2005). Maternal *torso* signaling controls body axis elongation in a short germ insect. *Curr. Biol.* **15**, 2131-2136.
Shimell, M. J., Ferguson, E. L., Childs, S. R. and O'Connor, M. B. (1991). The *Drosophila* dorsal-ventral patterning gene *tolloid* is related to human bone morphogenetic protein 1. *Cell* **67**, 469-481.
Shimmi, O., Umulis, D., Othmer, H. and O'Connor, M. B. (2005). Facilitated transport of a Dpp/Scw heterodimer by Sog/Tsg leads to robust patterning of the *Drosophila* blastoderm embryo. *Cell* **120**, 873-886.
Sprenger, F. and Nüsslein-Volhard, C. (1993). The terminal system of axis determination in the *Drosophila* embryo. In *The Development of Drosophila melanogaster*, Vol. 1 (ed. M. Bate and A. Martinez-Arias). Cold Spring Harbor, NY: Cold Spring Harbor Laboratory Press.
Stauber, M., Jäckle, H. and Schmidt-Ott, U. (1999). The anterior determinant *bicoid* of *Drosophila* is a derived Hox class 3 gene. *Proc. Natl. Acad. Sci. USA* **96**, 3786-3789.
Tautz, D. and Pfeifle, C. (1989). A non-radioactive in situ hybridization method for the localization of specific RNAs in *Drosophila* embryos reveals translational control of the segmentation gene *hunchback*. *Chromosoma* **98**, 81-85.
Umulis, D., O'Connor, M. B. and Blair, S. S. (2009). The extracellular regulation of bone morphogenetic protein signaling. *Development* **136**, 3715-3728.
Umulis, D. M., Serpe, M., O'Connor, M. B. and Othmer, H. G. (2006). Robust, bistable patterning of the dorsal surface of the *Drosophila* embryo. *Proc. Natl. Acad. Sci. USA* **103**, 11613-11618.
Umulis, D. M., Shimmi, O., O'Connor, M. B. and Othmer, H. G. (2010). Organism-scale modeling of early *Drosophila* patterning via bone morphogenetic proteins. *Dev. Cell* **18**, 260-274.
van der Zee, M., Stockhammer, O., von Levetzow, C., Nunes da Fonseca, R. and Roth, S. (2006). Sog/Chordin is required for ventral-to-dorsal Dpp/BMP transport and head formation in a short germ insect. *Proc. Natl. Acad. Sci. USA* **103**, 16307-16312.
Van der Zee, M., da Fonseca, R. N. and Roth, S. (2008). TGFbeta signaling in *Tribolium*: vertebrate-like components in a beetle. *Dev. Genes Evol.* **218**, 203-213.
Wang, Y.-C. and Ferguson, E. L. (2005). Spatial bistability of Dpp-receptor interactions during *Drosophila* dorsal-ventral patterning. *Nature* **434**, 229-234.
Wharton, K. A., Ray, R. P. and Gelbart, W. M. (1993). An activity gradient of *decapentaplegic* is necessary for the specification of dorsal pattern elements in the *Drosophila* embryo. *Development* **117**, 807-822.
Wiegmann, B. M., Trautwein, M. D., Winkler, I. S., Barr, N. B., Kim, J.-W., Lambkin, C., Bertone, M. A., Cassel, B. K., Bayless, K. M., Heimberg, A. M. et al. (2011). Episodic radiations in the fly tree of life. *Proc. Natl. Acad. Sci. USA* **108**, 5690-5695.

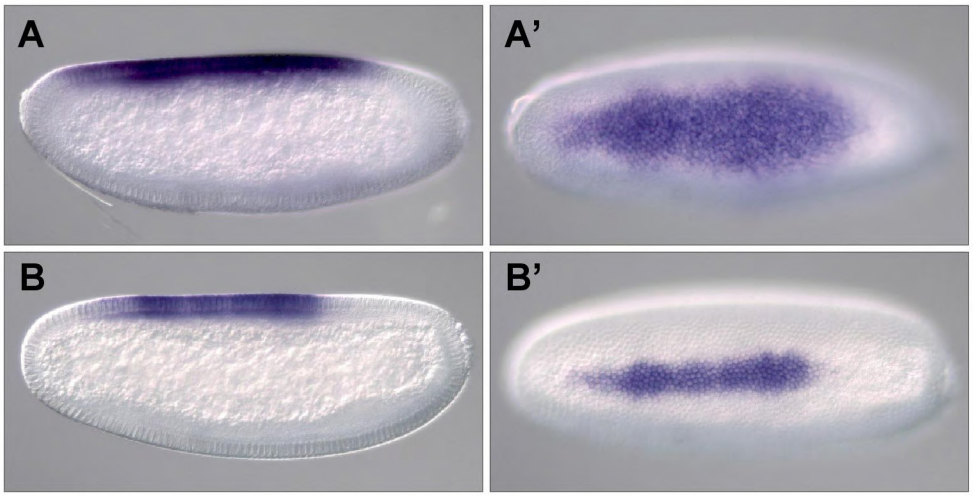

Fig. S1. *Mab-zen* expression dynamics in the blastoderm of *Megaselia abdita*. *Mab-zen* in situ hybridizations of two embryos at consecutive blastoderm cellularization stages are shown in (**A**,**B**) lateral and (**A′**,**B′**) dorsal view with anterior to the left.

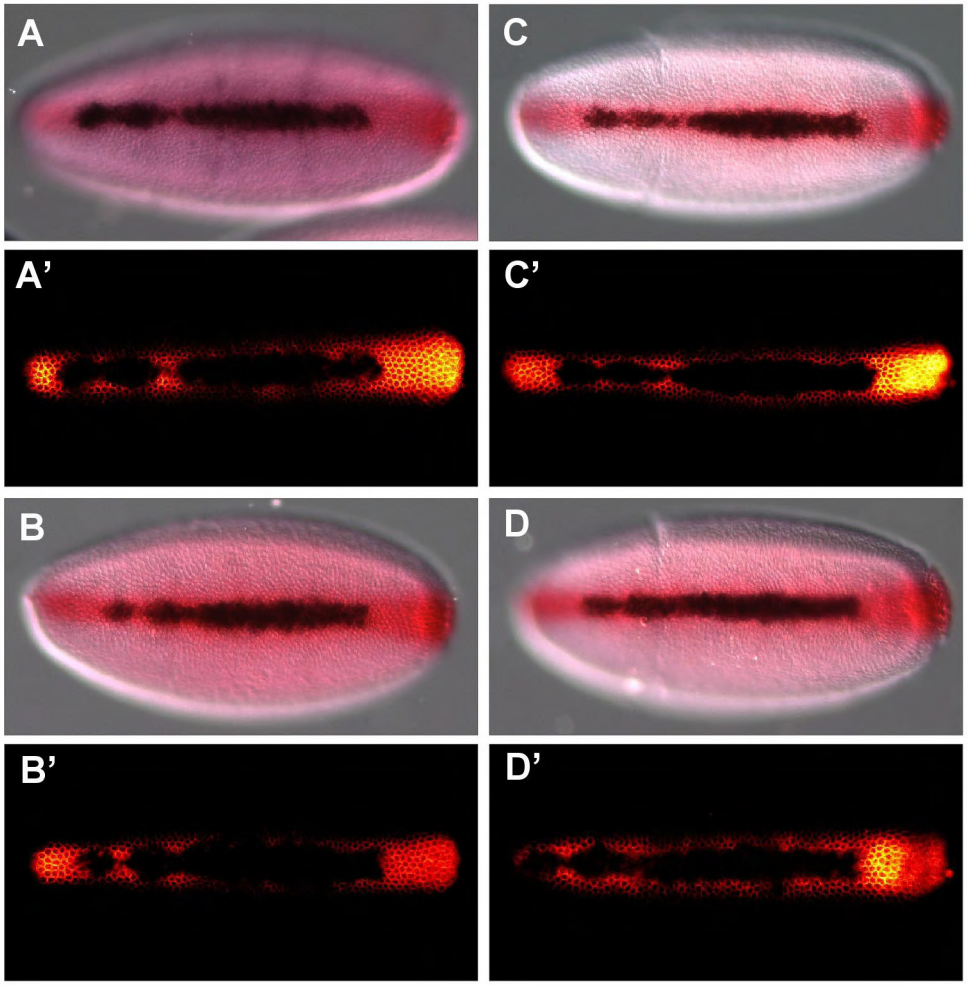

Fig. S2. pMad and *zen* transcript in *Drosophila melanogaster*. Double staining of pMad and *zen* transcript in *D. melanogaster* (**A-B′**) at the cellular blastoderm stage and (**C-D′**) during early gastrulation. All four embryos are shown in dorsal view with anterior to the left. *zen* transcript was detected using NBT/BCIP. pMad was detected using VectorRed and imaged in the Cy3 channel (A′-D′). NBT/BCIP quenches the pMad signal in the *zen* domain. Note that pMad is detected laterally adjacent to the *zen* domain, both shortly before and shortly after the onset of gastrulation.

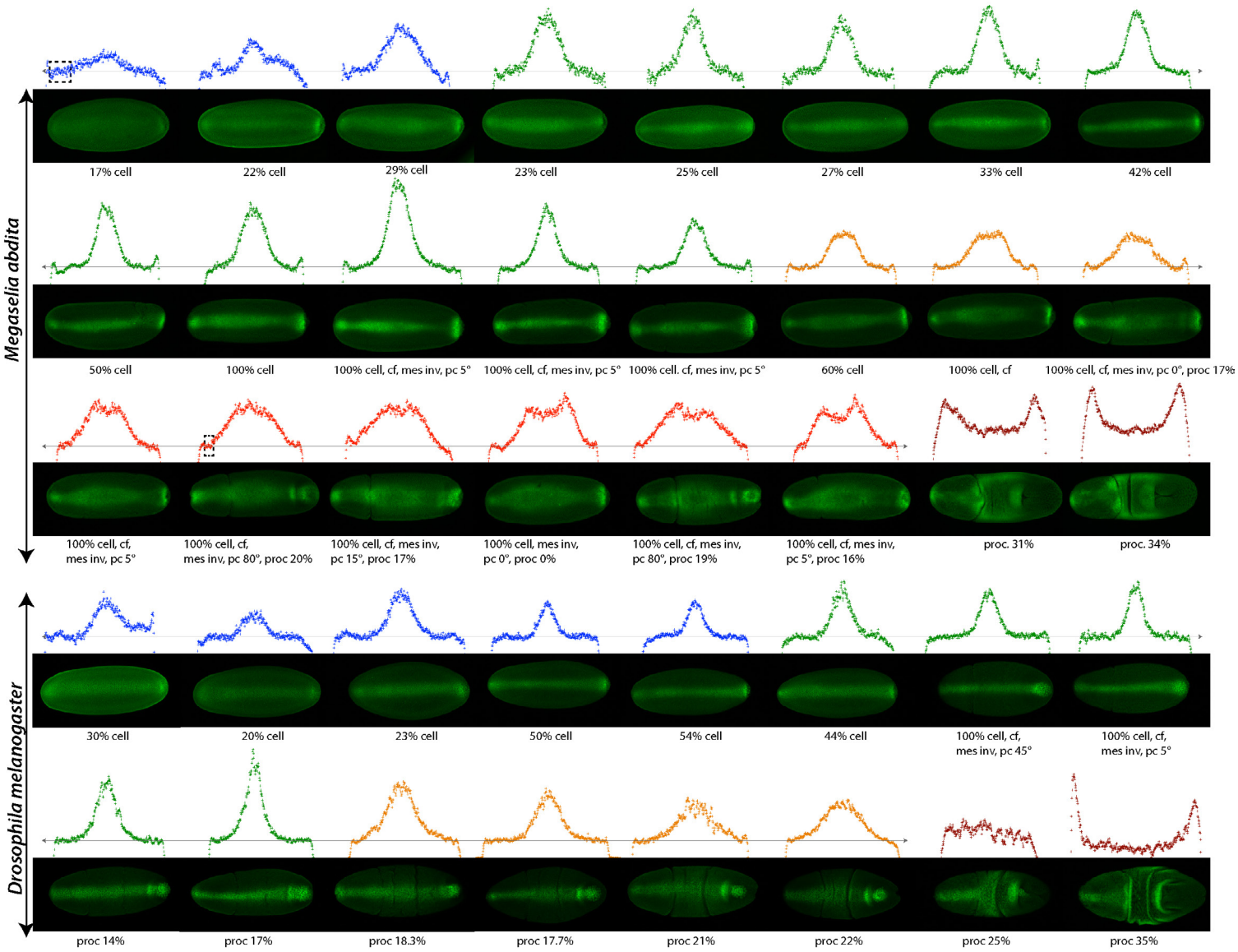

Fig. S3. pMad profiles of *M. abdita* and *D. melanogaster* embryos. Cross-sectional pMad profiles (at 50% egg length) of individual embryos are shown above dorsal projections of their confocal images. The embryos are shown in dorsal view with anterior to the left and grouped according to the shape of their pMad profiles as indicated by the color of the profile. Background intensity was calculated as the average intensity in the windows highlighted (dashed rectangles). All values in a profile were adjusted to these background values, which were treated as zero (gray line), except for profiles shown in dark brown (late gastrulation stages). Note the dorsocentral depression of pMad level in early gastrula stages of *M. abdita* (arrows), which is not conserved in *D. melanogaster*. Advanced gastrulation stages of both species exhibited an apparent reduction of the pMad level in the serosa of *M. abdita* or the amnioserosa of *D. melanogaster*, respectively. Abbreviations below images indicate morphological features of the respective embryos: cell, blastoderm cellularization; cf, cephalic furrow; mes inv, mesoderm invagination; pc, pole cell angle relative to length axis; proc, position of the proctodeum (see Materials and methods).

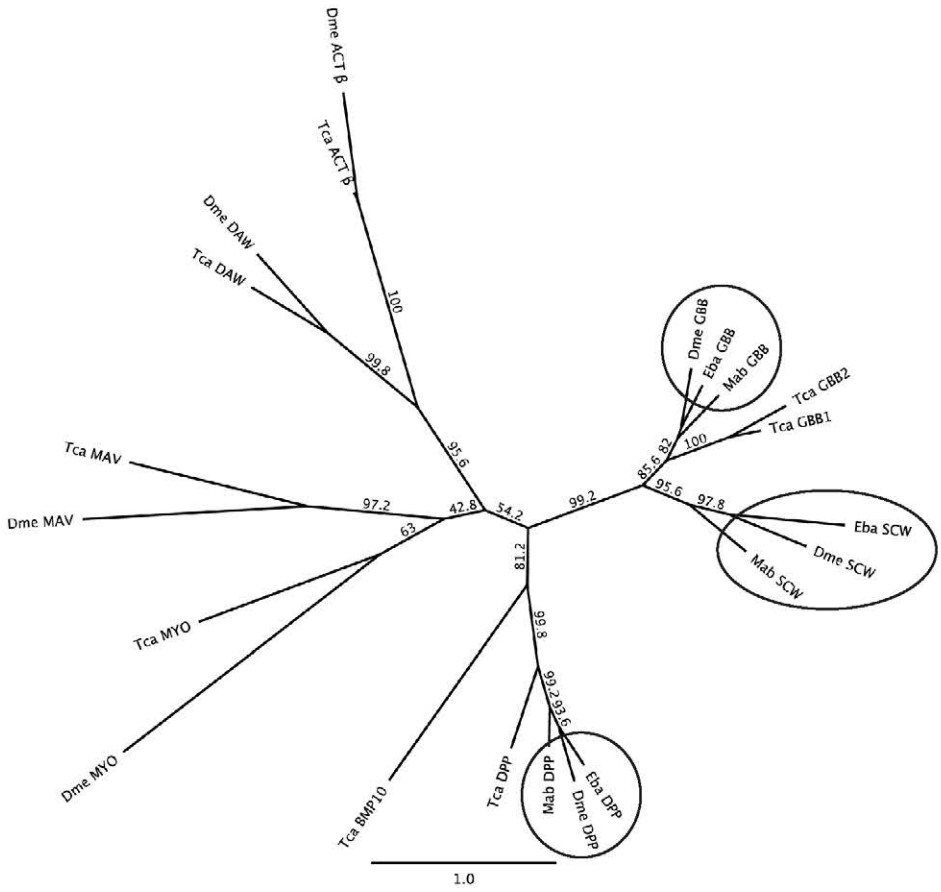
Dme ACT β
Tca ACT β
Dme DAW
Tca DAW
100
99.8
95.6
Tca MAV
Dme MAV
97.2
42.8
54.2
63
Tca MYO
Dme MYO
81.2
99.2
85.6 82
100
Dme GBB
Eba GBB
Mab GBB
Tca GBB2
Tca GBB1
95.6
97.8
Eba SCW
Dme SCW
Mab SCW
99.8
99.2 93.6
Tca BMP10
Tca DPP
Mab DPP
Eba DPP
Dme DPP
1.0

Figure S4A

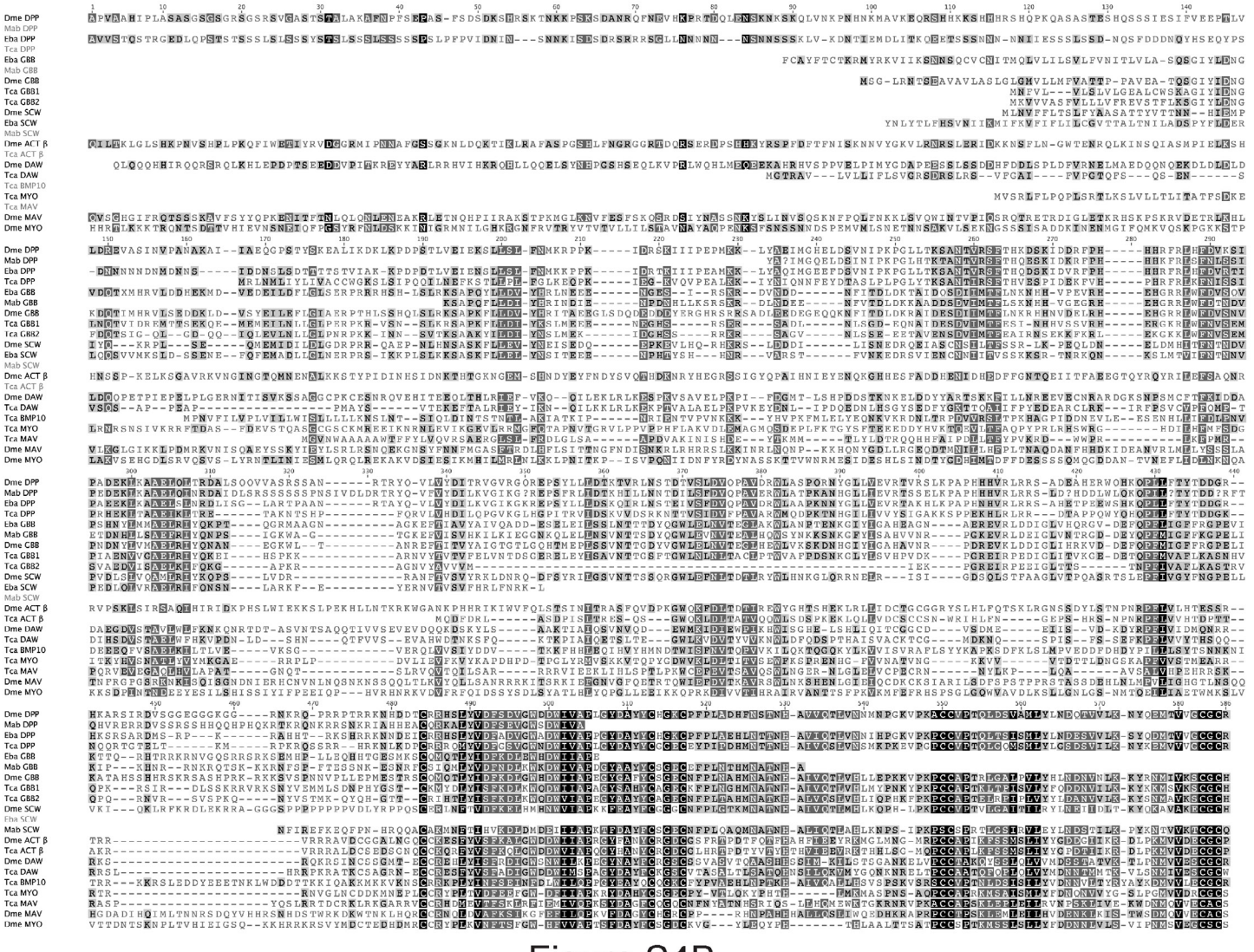

Figure S4B

Fig. S4. Phylogenetic analysis of BMP ligands. (**A**) Maximum likelihood tree of BMP ligand homologs of *Drosophila melanogaster* (*Dme*), *Episyrphus balteatus* (*Eba*), *Megaselia abdita* (*Mab*) and *Tribolium castaneum* (*Tca*). Homologs of Gbb, Scw and Dpp are circled. The gene tree was generated using the maximum likelihood method in PHYML with the Jones-Taylor-Thornton substitution model and 500 bootstrap iterations. The scale indicates one amino acid change per position. (**B**) ClustalW alignment of predicted protein sequences as used for tree building. Gap penalty was set to 3.0 and the extended gap penalty to 1.8. In the alignment, positions that were represented in less than 20% of the sequences and not conserved have been deleted manually. Highlighting indicates similarity to the consensus sequence using Blosum62 similarity matrix and threshold of 1; black, 100%; dark gray, 80% to <100%; light gray, 60% to <80%; unmarked, <60%.

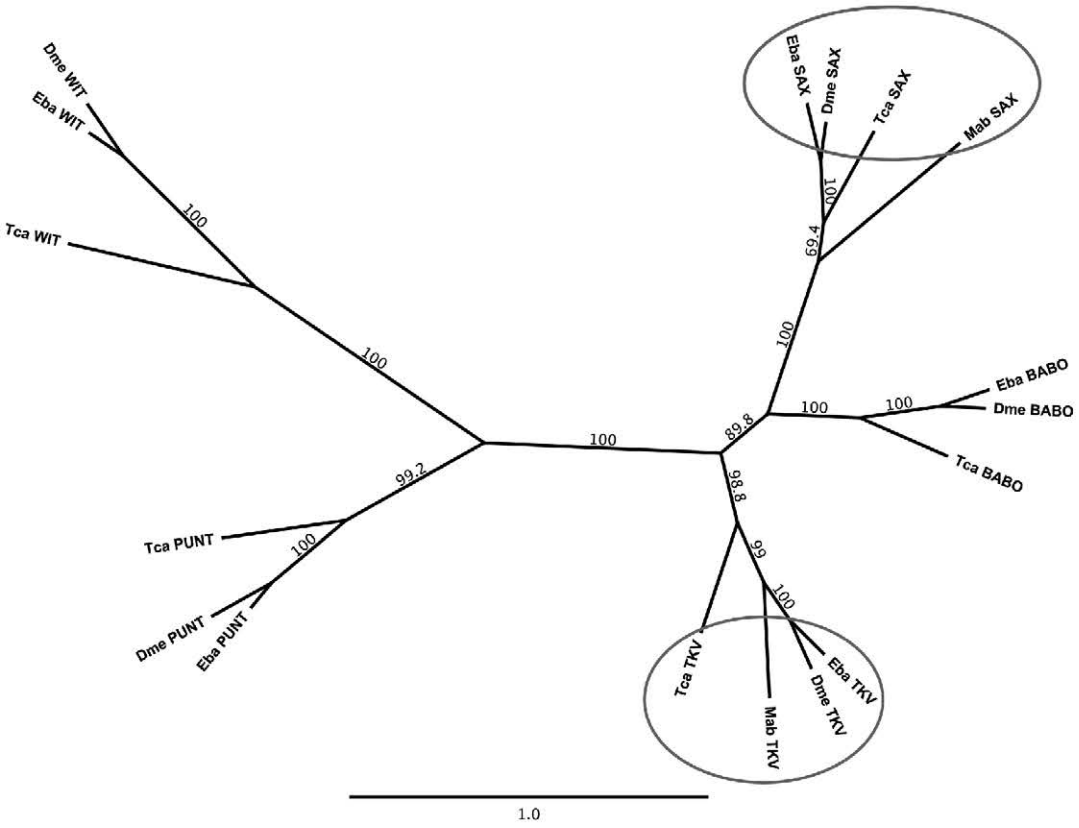
Dme WIT
Eba WIT
Tca WIT
Tca PUNT
Dme PUNT
Eba PUNT
Eba SAX
Dme SAX
Tca SAX
Mab SAX
Eba BABO
Dme BABO
Tca BABO
Tca TKV
Mab TKV
Eba TKV
Dme TKV
100
100
100
99.2
100
100
89.8
100
100
100
69.4
100
98.8
99
100
1.0

Figure S5A

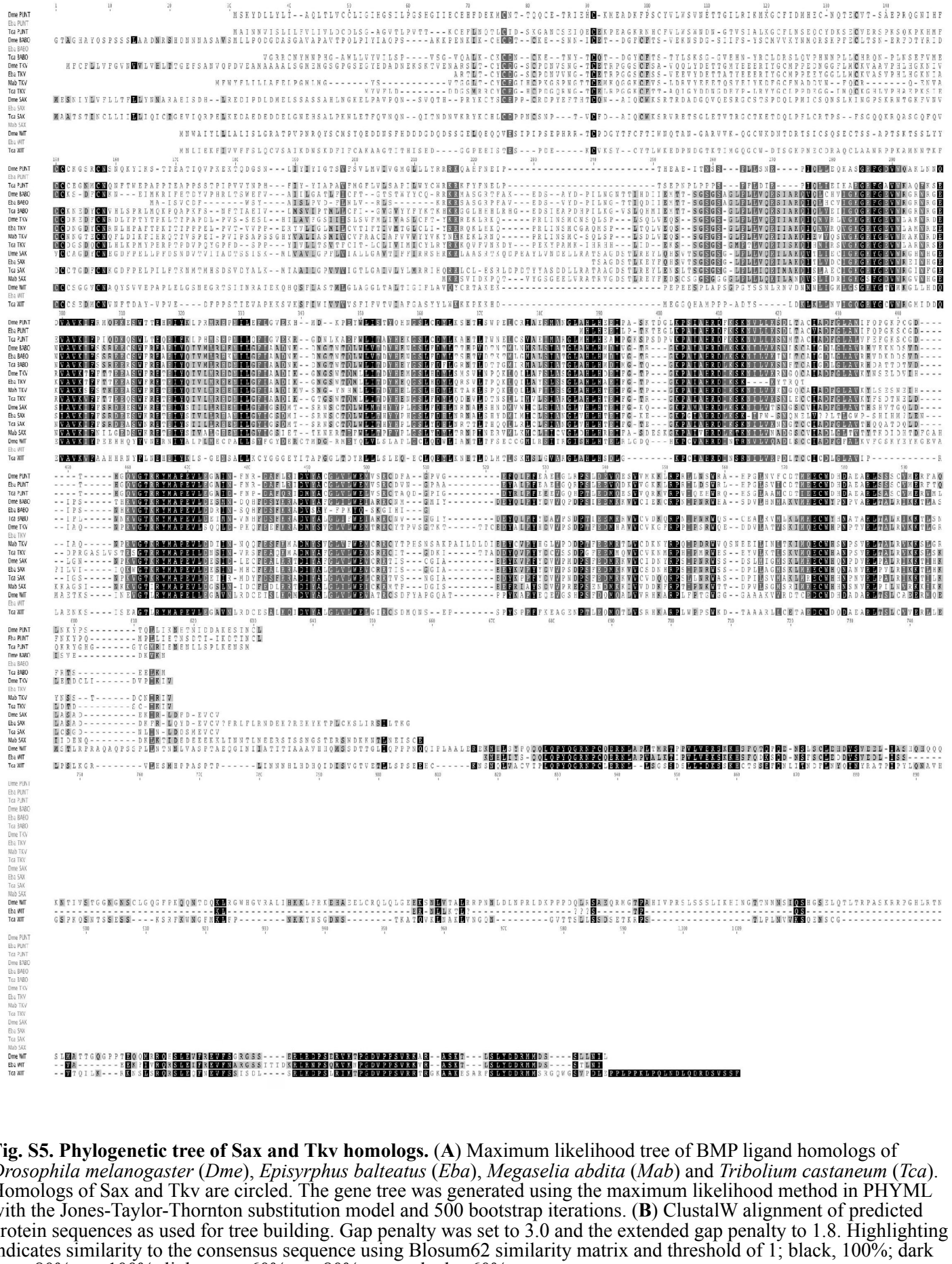

Fig. S5. Phylogenetic tree of Sax and Tkv homologs. (**A**) Maximum likelihood tree of BMP ligand homologs of *Drosophila melanogaster* (*Dme*), *Episyrphus balteatus* (*Eba*), *Megaselia abdita* (*Mab*) and *Tribolium castaneum* (*Tca*). Homologs of Sax and Tkv are circled. The gene tree was generated using the maximum likelihood method in PHYML with the Jones-Taylor-Thornton substitution model and 500 bootstrap iterations. (**B**) ClustalW alignment of predicted protein sequences as used for tree building. Gap penalty was set to 3.0 and the extended gap penalty to 1.8. Highlighting indicates similarity to the consensus sequence using Blosum62 similarity matrix and threshold of 1; black, 100%; dark gray, 80% to <100%; light gray, 60% to <80%; unmarked, <60%.

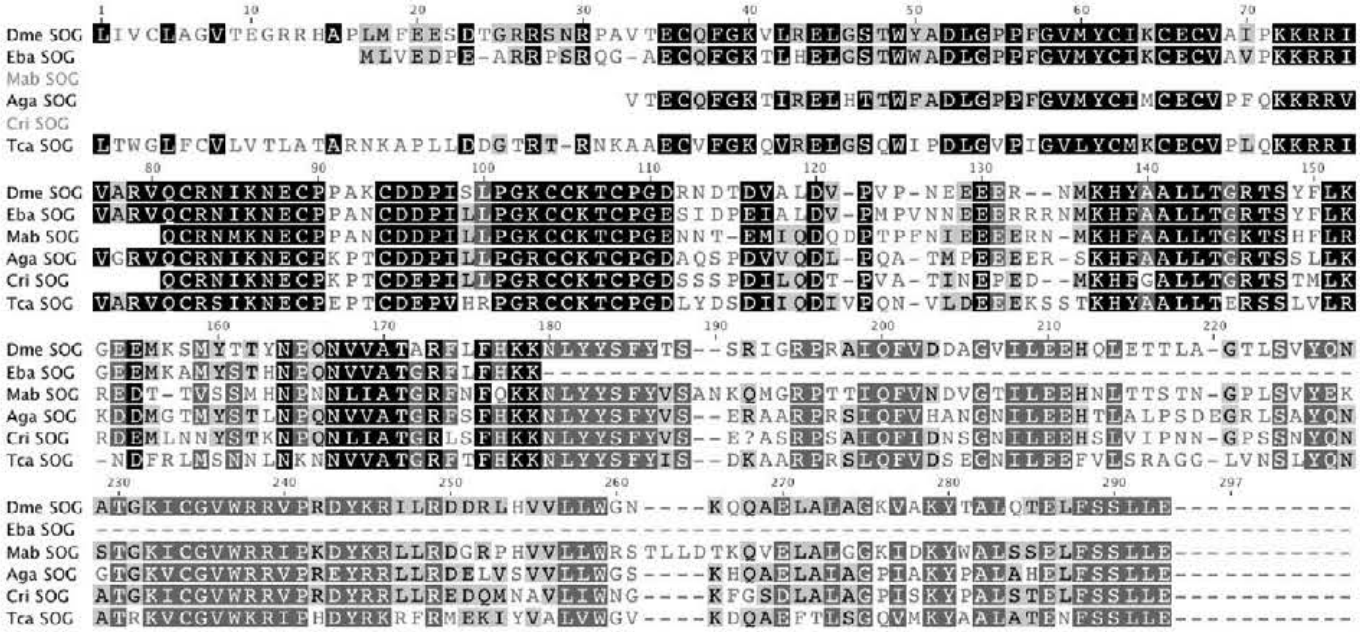

Fig. S6. Amino acid sequence alignment of Sog homologs. Truncated ClustalW alignment of predicted protein sequences of *Drosophila melanogaster* (*Dme*), *Episyrphus balteatus* (*Eba*), *Megaselia abdita* (*Mab*), *Chironomus riparius* (*Cri*) and *Tribolium castaneum* (*Tca*). Highlighting indicates similarity to the consensus sequence using Blosum62 similarity matrix and threshold of 1; black, 100%; dark gray, 80% to <100%; light gray, 60% to <80%; unmarked, <60%.

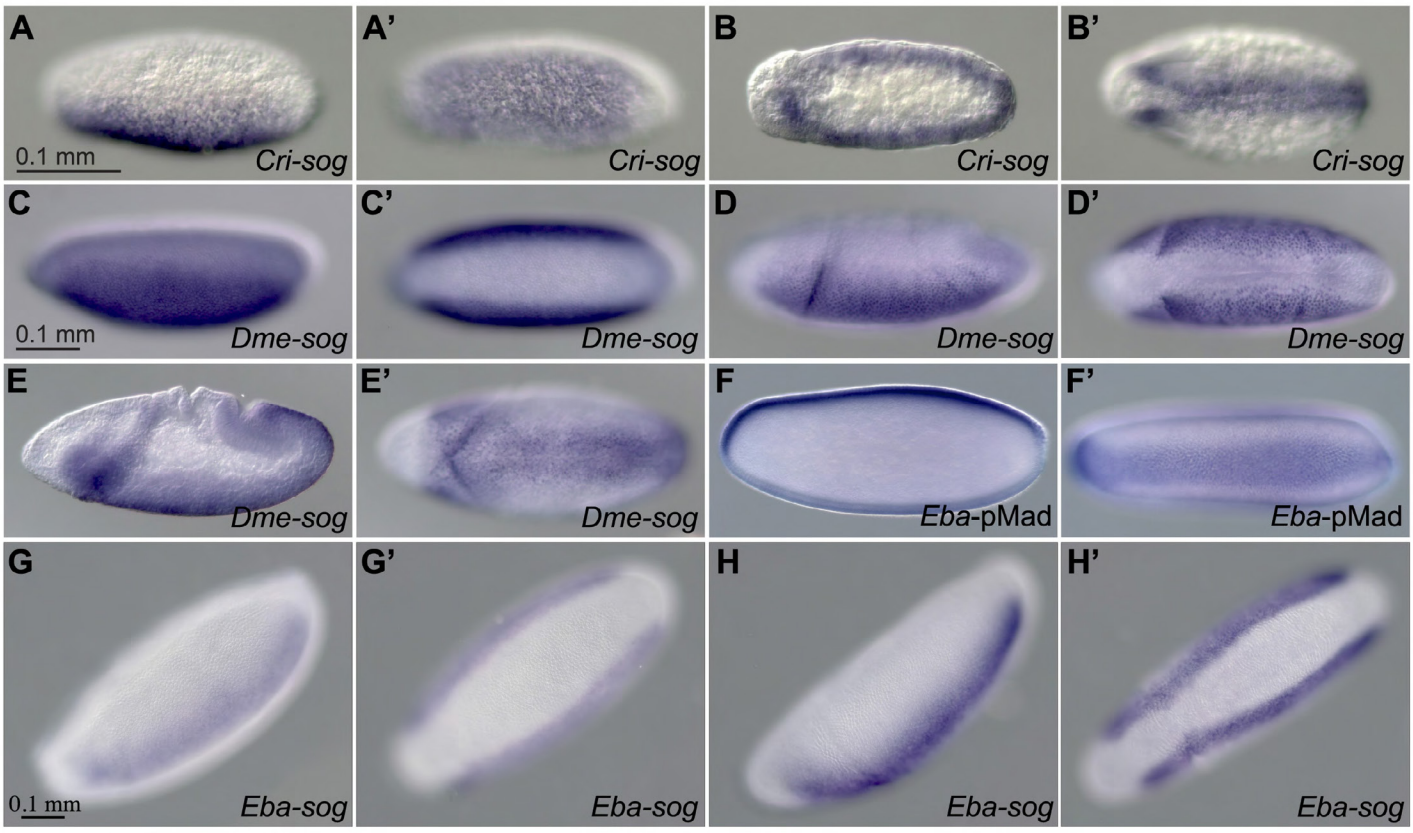

Fig. S7. Expression of *sog* in *Chironomus riparius* and *Drosophila melanogaster*, and pMad distribution and *sog* expression in *Episyrphus balteatus* (Syrphidae). (**A-B′**) *sog* in situ hybridizations at the blastoderm stage (A,A′) and the extended germband stage (B,B′) in *C. riparius*. (**C-E′**) *sog* in situ hybridizations at the blastoderm stage (C,C′) and consecutive gastrulation stages (D-E′) in *D. melanogaster*. (**F**,**F′**) pMad at the blastoderm stage in *E. balteatus*. (**G-H′**) *sog* in situ hybridizations at the blastoderm stage (G,G′) and at the beginning of gastrulation (H,H′) in *E. balteatus*. The embryos are shown in lateral view with the dorsal side up (A-H), or ventral view (A′-E′,G′,H′) or dorsal view (F′). Anterior is left.